



## TXM peptides inhibit SARS-CoV-2 infection, syncytia formation, and lower inflammatory consequences

Tea Govednik<sup>a,b</sup>, Duško Lainšček<sup>a,c</sup>, Urška Kuhar<sup>d</sup>, Marva Lachish<sup>e</sup>, Sandra Janežič<sup>f</sup>, Malan Štrbenc<sup>g</sup>, Uroš Krapež<sup>h</sup>, Roman Jerala<sup>a,c</sup>, Daphne Atlas<sup>e,\*\*</sup>, Mateja Manček-Keber<sup>a,c,\*</sup>

<sup>a</sup> Department of Synthetic Biology and Immunology, National Institute of Chemistry, 1000, Ljubljana, Slovenia

<sup>b</sup> Graduate School of Biomedicine, University of Ljubljana, 1000, Ljubljana, Slovenia

<sup>c</sup> Centre of Excellence EN-FIST, 1000, Ljubljana, Slovenia

<sup>d</sup> Institute for Microbiology and Parasitology, Veterinary Faculty, University of Ljubljana, 1000, Ljubljana, Slovenia

<sup>e</sup> Hebrew University of Jerusalem, Jerusalem, 91904, Israel

<sup>f</sup> National Laboratory of Health, Environment and Food, 2000, Maribor, Slovenia

<sup>g</sup> Institute for Preclinical Sciences, Veterinary Faculty, University of Ljubljana, 1000, Ljubljana, Slovenia

<sup>h</sup> Institute of Poultry, Birds, Small Mammals and Reptiles, Veterinary Faculty, University of Ljubljana, 1000, Ljubljana, Slovenia

### ARTICLE INFO

#### Keywords:

SARS-CoV-2

Disulfides

Thiol-reacting compound

Spike

Anti-inflammatory activity

### ABSTRACT

After three years of the SARS-CoV-2 pandemic, the search and availability of relatively low-cost benchtop therapeutics for people not at high risk for a severe disease are still ongoing. Although vaccines and new SARS-CoV-2 variants reduce the death toll, the long COVID-19 along with neurologic symptoms can develop and persist even after a mild initial infection. Reinfections, which further increase the risk of sequelae in multiple organ systems as well as the risk of death, continue to require caution. The spike protein of SARS-CoV-2 is an important target for both vaccines and therapeutics. The presence of disulfide bonds in the receptor binding domain (RBD) of the spike protein is essential for its binding to the human ACE2 receptor and cell entry. Here, we demonstrate that thiol-reducing peptides based on the active site of oxidoreductase thioredoxin 1, called thioredoxin mimetic (TXM) peptides, can prevent syncytia formation, SARS-CoV-2 entry into cells, and infection in a mouse model. We also show that TXM peptides inhibit the redox-sensitive HIV pseudotyped viral cell entry. These results support disulfide targeting as a common therapeutic strategy for treating infections caused by viruses using redox-sensitive fusion. Furthermore, TXM peptides exert anti-inflammatory properties by lowering the activation of NF- $\kappa$ B and IRF signaling pathways, mitogen-activated protein kinases (MAPKs) and lipopolysaccharide (LPS)-induced cytokines in mice. The antioxidant and anti-inflammatory effects of the TXM peptides, which also cross the blood-brain barrier, in combination with prevention of viral infections, may provide a beneficial clinical strategy to lower viral infections and mitigate severe consequences of COVID-19.

### 1. Introduction

The rapid spread of coronavirus disease (COVID-19) swiftly led to a global public health and societal crisis. Licensed vaccines show high efficacy and safety, but due to the high transmission rate and emerging immune-evading variants of SARS-CoV-2, the search for COVID-19 and future coronaviral therapeutics continues. Despite many efforts, the availability of specific drugs for mild cases, which are required for a faster recovery and preventing long-term COVID-19 symptoms, is limited. Since the interaction between the SARS-CoV-2 spike protein and

human angiotensin-converting enzyme-2 (ACE2) receptor is crucial for viral entry, interference with viral binding represents an important therapeutic strategy. Today, the majority of vaccines and antibodies are targeted toward viral spike protein (Zhou et al., 2021).

During viral infection, the SARS-CoV-2, like many other viruses, triggers oxidative stress, causing an excess of reactive-oxygen-species (ROS) and reactive-nitrogen-species (RNS), which interrupt the redox balance and further enhances redox-dependent viral infection (Suhail et al., 2020). In the COVID-19 pathophysiology, oxidative stress seems to be involved in other cellular processes, including hyperinflammation, coagulopathy, and hypoxia (van Eijk et al., 2021). Moreover, certain

\* Corresponding author. National Institute of Chemistry, Hajdrihova 19, 1000, Ljubljana, Slovenia.

\*\* Corresponding author.

E-mail addresses: [daphne.atlas@mail.huji.ac.il](mailto:daphne.atlas@mail.huji.ac.il) (D. Atlas), [mateja.mancek@ki.si](mailto:mateja.mancek@ki.si) (M. Manček-Keber).

<https://doi.org/10.1016/j.antiviral.2024.105806>

Received 7 July 2023; Received in revised form 23 December 2023; Accepted 8 January 2024

Available online 9 January 2024

0166-3542/© 2024 The Authors. Published by Elsevier B.V. This is an open access article under the CC BY-NC license (<http://creativecommons.org/licenses/by-nc/4.0/>).

### Abbreviations

ACE2	angiotensin-converting enzyme-2
AD4/NACA	N-acetyl cysteine amide
BAL	bronchoalveolar lavage
BFP	blue fluorescent protein
CXCL10	chemokine interferon- $\gamma$ inducible protein
GFP	green fluorescent protein
GSH	reduced glutathione
LPS	lipopolysaccharide
MAPKs	mitogen-activated protein kinases
NAC	N-acetylcysteine
RBD	receptor binding domain
RBM	receptor binding motif
RFP	red fluorescent protein
RNS	reactive nitrogen species
ROS	reactive oxygen species
TMPRSS2	transmembrane protease serine 2
TXM	thioredoxin mimetic
VSV	vesicular stomatitis virus

pre-existing conditions such as cancer, diabetes mellitus, and cardiovascular diseases, which are accompanied by elevated oxidative stress, increase the risk of developing severe infection. The viral receptor ACE2 plays a critical role in lowering oxidative stress. The binding of SARS-CoV-2 spike protein to ACE2 might also increase the cellular concentration of angiotensin II and elevate levels of superoxide species. Indeed, antioxidants such as N-acetylcysteine (NAC), reduced glutathione (GSH), polyphenols, vitamins C, D, and E, and selenium have been proposed to improve COVID-19 outcomes (Suhail et al., 2020).

In addition to preventing oxidative stress-related disorders through a reducing activity, antioxidants are beneficial also in preventing virus cell entry. Cell fusion is affected indirectly by the redox potential, mainly due to changes in the thiol-disulfide equilibrium of the receptor-binding-domain (RBD) of the spike protein (Manček-Keber et al., 2021). Other well-documented redox-sensitive viral fusion proteins are found in HIV, murine leukemia virus, human T-cell lymphotropic virus, rubella virus, Sindbis virus, and bovine viral diarrhoea virus (Anthony et al., 1992; Barbouche et al., 2003; Gros et al., 1997; Krey et al., 2005; Pinter et al., 1997; Wallin et al., 2004). In addition, cell entry of mouse-hepatitis virus, a member of the *Coronaviridae* family, has been shown to be inhibited by the free sulfhydryl compound (Sturman et al., 1990). Molecular dynamics simulations suggested that reducing all the disulfide bonds in both spike and ACE2 receptor to free thiol groups could impair binding affinity (Hati and Bhattacharyya, 2020). Preservation of disulfide-thiol balance within the spike protein has been suggested to be crucial for SARS-CoV-2 fusion and cell entry (Fraternal et al., 2023; Grishin et al., 2022; Khanna et al., 2022; Shi et al., 2022; Singh et al., 2020). Also, mutations of selected cysteine (Cys) residues in RBD lead to cell fusion inhibition, confirming the importance of disulfide integrity within the spike protein (Manček-Keber et al., 2021; Murai et al., 2022).

Spike protein forms a homotrimer, and each protomer consists of two proteolytic fragments, which are required for a successful cell entry. The RBD is part of the S1 subunit, while membrane fusion depends on the S2 subunit (Huang et al., 2020). SARS-CoV-2 spike protomers are rich in Cys residues, which are structurally important for viral activity, and many form disulfide bonds (Grishin et al., 2022). In RBD, four disulfide bridges are formed between Cys residues. Three pairs of Cys residues are localized in the core protein and help to stabilize the structure (Cys336-Cys361, Cys379-Cys432, Cys391-Cys525). The fourth pair is located in the receptor-binding motif (RBM) (Cys480-Cys488), the region that directly binds to the host receptor (Lan et al., 2020). Disulfide

bonds in RBD play a critical role in maintaining its proper structure, which is required for high-affinity interaction with the ACE2 receptor (Grishin et al., 2022; Singh et al., 2020). Several reducing agents and thiol-active compounds have already been demonstrated to inhibit viral entry. For example, N-acetylcysteine amide (AD4/NACA), JTT-705, and others, which have been shown to hinder the formation of syncytia of cells expressing spike protein, viral entry into host cells, and infection in a mouse model (Manček-Keber et al., 2021). In addition, tris (2-carboxyethyl) phosphine (TCEP) and dithiothreitol (DTT) inhibited viral replication at low millimolar levels (Grishin et al., 2022). Additionally, thiol-based reagents were shown to be effective in preventing coronavirus infection (Fraternal et al., 2023; Khanna et al., 2021; Shi et al., 2022).

Here, we present inhibition of SARS-CoV-2 entry into the cell by tri- and tetra-N- and C-blocked peptides consisting of two Cys residues. The peptides that mimic thioredoxin activity, and are termed thioredoxin mimetic (TXM) peptides, have been shown to be significantly more potent than NAC or NAC-amide (AD4/NACA) (Atlas, 2021; Bachnoff et al., 2011; Bartov et al., 2006). In addition to the redox activity and anti-inflammatory characteristics, the TXM peptides have been demonstrated to lower ROS accumulation, restore GSH, inhibit NF- $\kappa$ B nuclear translocation, and inhibit the MAPK induced inflammatory pathways (Canesi et al., 2019; Cohen-Kutner et al., 2013; Hemling et al., 2020; Kim et al., 2011). Here we show that TXM-CB3, TXM-CB12, TXM-CB13, TXM-CB30, and SD peptides, which act as antioxidants and anti-inflammatory reagents (Baratz-Goldstein et al., 2016; Kim et al., 2011; Lejnevic et al., 2016; Wiesen and Atlas, 2022), also prevent binding of SARS-CoV-2 spike protein to the receptor, cell fusion and cell entry of several SARS-CoV-2 viral strains. Furthermore, TXM peptides prevent SARS-CoV-2 and also HIV gp160 pseudovirus cell infection. In vivo, the peptides effectively lower pseudovirus infection as well as lipopolysaccharide (LPS)-induced inflammation. Altogether, these findings demonstrate the efficiency of TXM peptides in inhibiting viruses that exhibit thiol/disulfide rearrangements of fusion proteins for cell entry, and the ability to combat cellular inflammation and oxidative stress. Future emergence of new variants of concern that maintain the ability to tightly bind the ACE2 receptor might resist monoclonal anti-COVID-19 antibodies. Therefore, TXM peptides could become a potential therapeutic strategy for treating viral infection concomitantly with lowering oxidative stress and inflammatory consequences.

## 2. Materials and methods

### 2.1. Peptides

N-acetylcysteine amide (AD4/NACA) and the thioredoxin mimetic (TXM) peptides TXM-CB3, TXM-CB12, TXM-CB13, TXM-CB30, and SD were custom synthesized by Novetide Ltd. Haifa (Israel). Synthesized peptides were analyzed by mass spectrometry, and HPLC purified to achieve the following purity: AD4/NACA >98 %, CB3 98 %, CB12 97.5 %, CB13 97.3 %, CB30 > 95 %, and SD > 95 %. Auranofin was purchased from Enzo Life Sciences (Shoham, Israel). All compounds are water-soluble and were dissolved in ultra-pure water.

### 2.2. Pseudovirus assay

The effect of compounds on virus entry was tested using a pseudovirus system based on the vesicular stomatitis virus (VSV) as formerly described (Lainšček et al., 2021; Manček-Keber et al., 2021). During the production of SARS-CoV-2 pseudovirus, HEK293T pseudovirus-producing cells were transfected with pCG1-Spike. For HIV pseudovirus production, HEK393T pseudovirus-producing cells were transfected with HIV-AC10.0.29 Env plasmid. For the SARS-CoV-2 pseudovirus assay, one-day pre-transfection HEK293 cells were seeded ( $2.5 \times 10^4$  per well) in a 96-well plate in DMEM + 10 % FBS medium. Transfection with a pCG1-hACE2 plasmid (0.02  $\mu$ g) and a plasmid

encoding Renilla luciferase phRL-TK (Invitrogen) was carried out using Lipofectamine 2000 (Invitrogen). For the HIV pseudovirus assay, CD4 and CCR5 receptor expressing U87 stable cell line (U87.CD4.CCR5) was used.

Next we explored whether the TXM peptides affect virus entry acting extracellularly or intracellularly. The extracellular activity was tested by incubation of the pseudovirus with the TXM peptides for 30 min, and then the pseudovirus was added to the cells. The peptide solvent was used as a negative control. The intracellular activity of the peptides was tested in cells that were incubated first for 60 min with the corresponding compounds, and washed with medium before pseudovirus infection. In both cases, the pseudovirus-containing medium was removed the following day, and the cells were lysed in a Passive lysis buffer (Biotium). The activity of firefly luciferase of pseudovirus infection was determined after the addition of luciferin substrate (Xenogen). *Renilla* luciferase activity was measured after the addition of coelenterazine H (Xenogen) and then used for normalization. Luciferase measurements were performed on the luminometer Orion (Berthold Technology).

### 2.3. Surrogate assay of pseudovirus infection

All animal studies were performed according to the directives of the EU 2010/63 and were approved by the Administration of the Republic of Slovenia for Food Safety, Veterinary and Plant Protection of the Ministry of Agriculture, Forestry and Foods, Republic of Slovenia (Permit Number U34401-6/2021/5). The inhibitory effect was tested on thirty female 10-week old Balb/c OlaHsd mice (Envigo, Italy). All animals used in the study were healthy and accompanied by health certificates from the animal vendor. Mice were housed in IVC cages (Techniplast, Italy) with wood fiber bedding (Mucedola) and maintained in a 12-12 dark-light cycle. Animals were fed standard chow (4RF21, Mucedola) and provided with tap water ad libitum. Six mice were used for each tested group to obtain statistically relevant results.

On days 1 and 2, mice were injected intraperitoneally (250  $\mu$ L/animal) with the TXM peptides (2 mg/mouse/day) dissolved in ultra-pure water. On day 2, mice were also transfected with a mixture (50  $\mu$ L) of in vivo-jetPEI transfection reagent (Polyplus) and plasmid DNA with the N/P ratio 7. Each animal received 22  $\mu$ g plasmid DNA (20  $\mu$ g pCG1-hACE2 and 2  $\mu$ g pCMV3-c-Myc-TMPRSS2) combined with the transfection reagent via intranasal administration. On day 3, mice were intranasally infected with 60  $\mu$ L of VSV $\Delta$ G SARS-CoV-2 pseudovirus. On day 4, mice subcutaneously received 150 mg/kg of body weight of D-luciferin (Xenogen) and were imaged in vivo using IVIS Lumina Series III (Perkin Elmer). Bioluminescence that depicted the state of pseudovirus infection was determined. Values of mice background were subtracted from bioluminescence values. Data were analyzed using Living Image 4.5.2 (Perkin Elmer).

### 2.4. SARS-CoV-2 virus isolation and in vitro cell infection

The patient-derived SARS-CoV-2 strain Slovenia/SI-4265/20, D614G was provided by the European Virus Archive. SARS-CoV-2 variants Alpha/B.1.1.7 (GISAID: EPI\_ISL\_1240614), Delta/B.1.617.2 (AY.98.1) (GISAID: EPI\_ISL\_3061362), and Omicron/BA.5.2.1 (GISAID: EPI\_ISL\_15111405) were isolated at the Institute of Microbiology and Parasitology, Veterinary Faculty, University of Ljubljana from samples collected by the National Laboratory for Health, Environment and Food from SARS-CoV-2 positive individuals. Virus isolation and preparation of virus stocks for further experiments were performed on Vero E6 cells in a biosafety level 3 laboratory as previously described (Janezic et al., 2023).

For the in vitro cell infection, one day before infection, Vero E6 cells were seeded into a 96-well plate at a density of  $3.5 \times 10^4$  cells per well in an Eagle's Minimum Essential Medium (EMEM, ATCC 30-2003) containing 10 % FBS (Gibco) at 37 °C in 5 % CO<sub>2</sub> incubator. To explore

differences in intracellular and extracellular activity of the TXM peptides, the inhibitory effect was tested with two different protocols: 1) The compound was incubated with the virus for 1 h prior to cell infection. Cells were washed with EMEM, and virus inoculum was added. After 1 h of infection, the cells were rewashed and incubated overnight in EMEM containing the indicated amount of tested compound. 2) Cells were washed with EMEM, and virus inoculum was added. After 1 h of infection, the cells were washed and incubated overnight with EMEM containing the tested compound at the indicated concentrations. The next day, the cells were washed twice with EMEM. A synthetic trypsin TrypLE™ Express Enzyme (1X) in phenol red (Gibco) was used to detach the cells, which were used for RNA isolation using the MagMAX™ CORE Nucleic Acid Purification Kit on the KingFisher Flex System (Thermo Fisher Scientific). Viral RNA was measured with the real-time RT-qPCR assay targeting the E gene of SARS-CoV-2 using primers and probes as described by Corman et al. (2020). To detect GAPDH as endogenous control, we used TaqMan Gene Expression Assays from Applied Biosystems (Thermo Fisher Scientific, assay ID Rh02621745-g). For all RT-qPCR assays, AgPath-IDTM One-Step RT-qPCR Reagents (Thermo Fisher Scientific) were used. RT-qPCR was performed by QuantStudio 5 (Thermo Fisher Scientific) using 2  $\mu$ L of the extracted total RNA. After the exclusion of possible outliers (determined on  $\Delta$ Ct values with the IQR method), the results from RT-qPCR were analyzed based on  $2^{-\Delta\Delta Ct}$  method (Livak and Schmittgen, 2001) with a predisposition that RNA target and GAPDH reference had similar enough qPCR amplification conditions to allow pairing.

### 2.5. Oxidative stress assay

Rat pheochromocytoma (PC12) cells (undifferentiated) were cultured at 37 °C, 5 % CO<sub>2</sub> in DMEM supplemented with 10 % FBS, ampicillin, and streptomycin. Prior to the experiment, PC12 cells were plated at a density of  $8.5 \times 10^4$ /cm<sup>2</sup> on collagen (rat tail) (Roche Diagnostics) coated plates and incubated for 24 h. Cells were subjected to oxidative stress by incubation for 30 min at 37 °C with DMEM containing 5  $\mu$ M auranofin. Treatment with TXM-CB3 at the indicated concentrations consisted of a wash with PBS (Biological Industries) and incubation for 30 min with DMEM. Then, the cells were washed with ice-cold PBS and subsequently lysed in 0.1–1.5 ml ice-cold lysis buffer (150 mM Tris-HCl, pH 6.8, 10 % glycerol, 0.6 % SDS, bromophenol blue, supplemented with 7  $\mu$ L  $\beta$ -mercaptoethanol/ml). The cell lysates were collected and boiled at 100 °C for 5 min prior to protein separation.

Western blot analysis was performed essentially as previously published (Bachnoff et al., 2011). Twenty to thirty  $\mu$ g of protein samples were loaded on 10 or 12 % SDS-PAGE gels. The proteins were then transferred electrophoretically to the nitrocellulose membrane (Whatman). Prior to hybridization with antibodies, the nitrocellulose membranes were cut and blocked by incubation for 1 h at RT in TBS-T (25 mM Tris-HCl pH 7.4, 0.9 % NaCl, and 0.02 % Tween-20) with 4 % Difco skim milk (BD). Membranes were then incubated overnight at 4 °C with the primary antibody. Detection was performed using the corresponding antibodies pERK1/2 (Thr 202/Tyr204), mouse mAb; ERK2 (Santa Cruz) rabbit Ab; p-SAPK/JNK (Thr183/Tyr185), rabbit mAb; SAPK/JNK,  $\beta$ -catenin (BD biosciences Franklin Lakes, USA). Proteins were detected with anti-mouse or anti-rabbit IgG-HRP linked antibody (1:10,000; Cell Signaling Technology). The ratios of phosphorylated ERK1/2 and JNK to the  $\beta$ -catenin were calculated. The values shown for pERK1, pERK2, pJNK1, and pJNK 2 are averages ( $\pm$ SEM) based on 3 independent experiments, normalized to the phosphorylation state of cells treated with 5  $\mu$ M auranofin and plotted with a linear regression program.

### 2.6. NF- $\kappa$ B and IRF pathway induction

To further examine the anti-inflammatory effect of TXM peptides, A549-Dual™ cell line with two inducible reporters was used. Before the experiments, cells were first maintained in high glucose DMEM (Gibco)

with 10 % FBS supplemented with 10  $\mu\text{g/ml}$  of blasticidin (Invivogen) and 100  $\mu\text{g/ml}$  of Zeocin (Invivogen). Cells were seeded at  $1.7 \times 10^4$  per well in a 96-well plate in high glucose DMEM with 10 % FBS. The following day, cells were stimulated with poly (I:C) (2  $\mu\text{g/ml}$ ) (Invivogen) added directly into cell medium to be endocytosed and presented to TLR3 or transfected using DOTAP (Roche) (0.4  $\mu\text{g/ml}$  poly (I:C) with 0.03  $\mu\text{l}$  DOTAP per ng) to reach the cytoplasm for MDA5/RIG-I activation. Three hours after the stimulation, tested compounds were added at the indicated concentrations. Induction of reporters was measured 24 h post-stimulation. Interferon regulatory pathway (IRF) activation was determined by measuring the *Lucia* luciferase light units (LU) on Centro Microplate Luminometer (Berthold) using coelenterazine H (Xenogen) as substrate. Activation of NF- $\kappa$ B was determined using QUANTI-Blue (Invivogen), a SEAP detection reagent, by reading the optical density (OD) at 620 nm using a Microtiter plate reader Sinergy Mx (Biotek).

## 2.7. In vivo anti-inflammatory study

Experiments were performed by »Science in action«, Ltd; Ness-Ziona, Israel, that provides animal studies as an outsourcing service. All animals were treated according to the National Institute of Health (NIH) guidelines for the care and use of laboratory animals. The Animal Testing Council of the Ministry of Health in Israel accredits the company, and licensed veterinarians conducted the experiments (#C148210). Mice were sacrificed by an overdose of  $\text{CO}_2$  and decapitated.

Sixteen female BALB/c mice were anesthetized and orally intubated with a sterile plastic catheter and challenged with intratracheal instillation of 800  $\mu\text{g}$  of LPS dissolved in PBS (saline/LPS). Five mice were used as naïve controls. The anti-inflammatory activity of TXM-CB3 was determined in vivo in LPS-treated mice. Eight LPS-challenged mice were injected intravenously (i.v.) with TXM-CB3 dissolved in PBS 1.0 mg/mice (50 mg/kg) at 3 time points: 15 min prior to LPS, 24 h after LPS/saline, and 48 h after LPS. Mice were sacrificed 72 h after the LPS challenge to collect tissues for analysis. The effect on LPS-induced inflammatory damage was examined by the differential cell count of T-lymphocytes, B-lymphocytes, eosinophils, neutrophils, and monocytes/macrophages in the bronchoalveolar lavage (BAL) fluid by flow cytometry. Levels of cytokines, pro-inflammatory vs. anti-inflammatory, in BAL fluid were measured by ELISA.

## 2.8. Statistical analysis

GraphPad Prism 8 was used to generate figures and perform statistical analysis. Bar data from independent experiments are represented as mean  $\pm$  SEM. ANOVA with Dunnett's multiple comparison test or

Student's t-test was used for statistical analysis. Data for inhibition of viral entry and replication from a representative experiment are presented as mean fold change with an incorporated range of SD of the  $\Delta\Delta\text{Ct}$  values (bar plots) and  $\Delta\Delta\text{Ct} \pm \text{SD}$  (line graphs) (Livak and Schmittgen, 2001). For statistical analysis of RT-qPCR, Brown-Forsythe and Welch ANOVA test with Dunnett's multiple comparisons test was used on  $\Delta\text{Ct}$  values.  $\text{IC}_{50}$  values were determined using Hill equation and regression model, and are shown with corresponding SEM.

## 3. Results

### 3.1. Tri- and tetra-thioredoxin mimetic (TXM) peptides inhibit syncytia formation and binding of the SARS-CoV-2 spike protein to the ACE2 receptor

The RBD domain of the S1 subunit contains four Cys pairs, which are susceptible to the redox state of the extracellular medium, affecting spike protein and ACE2 binding (Fig. 1A). Aimed at converting the disulfide bonds at the RBD domain to the reduced form, several thiol-based molecules were tested, N-acetylcysteine amide (AD4/NACA) and the TXM peptides (Fig. 1B). AD4/NACA is the amide form of N-acetylcysteine (NAC), which compared to NAC is more potent and membrane-permeable (Atlas, 2021; Bartov et al., 2006; Grinberg et al., 2005; Offen et al., 2004). The TXM peptides represent a family of small molecular weight thiol-reducing peptides, designed based on the -Cys-X-X-Cys- and -Cys-X-Cys- motifs responsible for the redox activity of Trx1 and other oxidoreductases (Bachnoff et al., 2011; Bartov et al., 2006; Cohen-Kutner et al., 2013; Kim et al., 2011). The X within the -Cys-X-X-Cys- or -Cys-X-Cys- motifs could be any amino acid residue. By virtue of the two Cys residues, members of the tri- and tetra-TXM peptides, reduce protein disulfides, mimicking Trx1 activity.

Initially, the effect of the TXM peptides on spike protein binding to ACE2 was examined in ACE2-coated ELISA plates by incubation of the spike protein with increasing concentrations of the reducing peptides. AD4/NACA has previously been shown to be effective at millimolar concentrations and was used as a positive control (Manček-Keber et al., 2021).

As shown, AD4/NACA, TXM-CB3, TXM-CB12, TXM-CB13, TXM-CB30, and SD efficiently and dose-dependently inhibited spike-ACE2 interaction (Fig. 2A). All TXM peptides disrupted spike protein binding to the receptor at micromolar ( $\mu\text{M}$ ) concentrations, compared to AD4/NACA, which required a  $>10$ -fold higher concentration. These results demonstrate a higher efficiency of the Trx-based compounds, compared to AD4/NACA.

Cells expressing spike protein on the plasma membrane fuse with ACE2-expressing cells (Suppl. Fig. 1). Also, during SARS-CoV-2

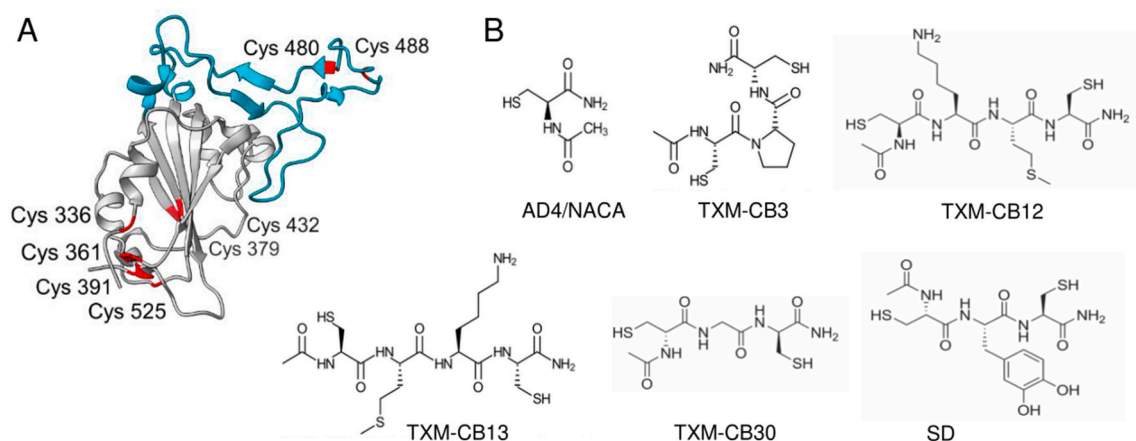


**Fig. 1.** Disulfide pairs in RBD of SARS-CoV-2 and thiol-reducing antioxidant compounds. (A) Schematic localization of Cys pairs (red) within the RBD and RBM (cyan) of SARS-CoV-2. (B) Chemical structures of AD4/NACA and thioridoxin mimetic (TXM) peptides TXM-CB3, TXM-CB12, TXM-CB13, TXM-CB30, and SD.

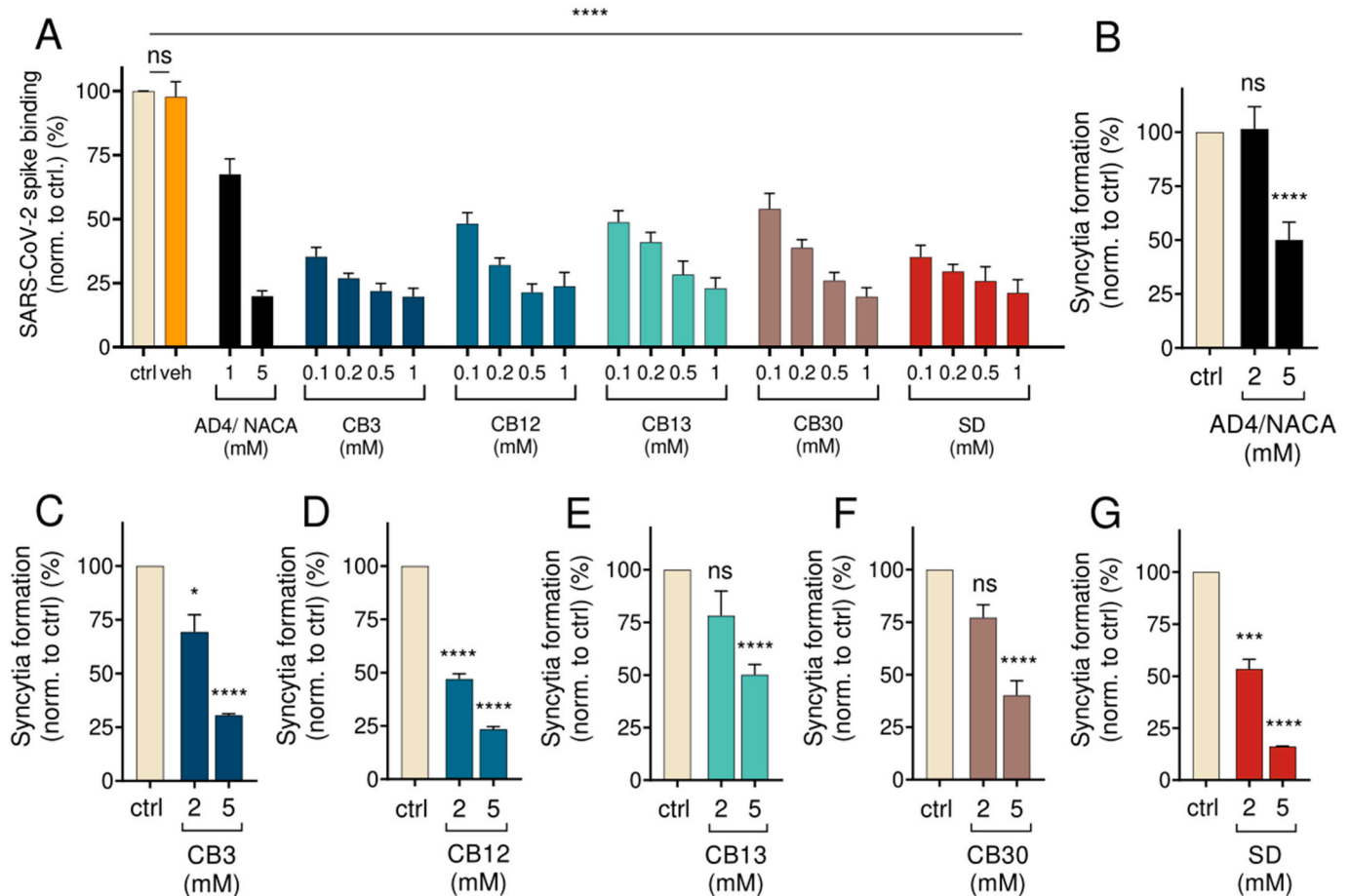


**Fig. 2. TXM peptides inhibit SARS-CoV-2 spike protein binding to ACE2 receptor and syncytia formation.** (A) Spike protein was incubated w/o compounds for 1 h and then added to ACE2-coated plates for 2 h. Bound spike protein was detected by absorbance using streptactin-HRP. Control is untreated spike (ctrl), vehicle is spike treated with peptide solvent (veh). (B–G) HEK293T cells were transfected with spike and cLuc:N7 or ACE2 receptor and nLuc:N8 plasmids. Spike-expressing cells were preincubated w/o compounds for 30 min and mixed with ACE2-expressing cells for 3 h. Reconstituted luciferase activity was determined. Combined means from at least three indep. exp. for ELISA and three indep. exp. for split luciferase assay are shown as mean  $\pm$  SEM. Comparison to untreated control (ctrl) was analyzed using one-way ANOVA with Dunnett's multiple comparison test. \*\*\*\*p < 0.0001; \*\*\*p < 0.001; \*p < 0.05; non significant (ns).

infection, these giant multinucleated cells called syncytia are formed and contribute to the pathogenicity of COVID-19, particularly in the lung (Bussani et al., 2020; Ou et al., 2020). Different levels of fusogenicity of SARS-CoV-2 variants are tightly correlated with pathogenicity. The Delta variant is highly fusogenic and notably more pathogenic, whereas variants such as omicron BA.1 that show impaired syncytia formation exert lower pathogenicity (Meng et al., 2022; Saito et al., 2022; Yamasoba et al., 2022).

A sensitive split luciferase reporter assay, based on N7/N8 coiled-coil peptide pair, was used to measure syncytia formation (Manček-Keber et al., 2021; Plaper et al., 2021). As shown, all TXM peptides inhibited syncytia formation (Fig. 2B–G) and were not toxic to the cells, determined by measuring 7-AAD staining after 3 h incubation (Suppl. Fig. 2). TXM-CB3 ( $IC_{50} = 2.05 \pm 0.14$  mM), TXM-CB12 ( $IC_{50} = 1.77 \pm 0.04$  mM), and SD ( $IC_{50} = 1.94 \pm 0.06$  mM) appeared to be most effective, exhibiting a stronger inhibition at lower applied concentrations than TXM-CB13 ( $IC_{50} = 2.17 \pm 0.29$  mM), TXM-CB30 ( $IC_{50} = 2.23 \pm 0.07$  mM), and NACA ( $IC_{50} = 3.32 \pm 0.54$  mM).

### 3.2. TXM peptides prevent a cell-fusion step more efficiently than preventing spike-ACE interaction

Flow cytometry was applied to distinguish between cells interacting through spike-ACE2 interactions and syncytia formation, which requires

membrane fusion (Manček-Keber et al., 2021). Briefly, spike-expressing cells were cotransfected with split GFP<sub>(1-10)</sub>;gs:N7 and iRFP<sup>NLS</sup>, whereas ACE2-expressing cells were cotransfected with split 3x(N8:g:GFP<sub>11</sub>) and BFP<sup>NLS</sup>. The population of double-positive BFP and iRFP cells represents cells that interact with each other and in which spike protein is bound to ACE2. Within a double-positive population, a subgroup of GFP-positive cells represents syncytia-forming cells (Suppl. Fig. 3). While the tested compounds did not alleviate interactions of spike-expressing cells with ACE2-expressing cells at the corresponding concentrations (5 mM) (Fig. 3A), they significantly inhibited syncytia formation, as shown by a substantial decrease in split GFP reconstitution (Fig. 3B and C). However, at higher concentrations of TXM-CB3 peptide (10, 20 and 40 mM) also interaction between spike-expressing cells and ACE2-expressing cells was mitigated (Fig. 3D), confirming TXM peptide mode of action. TXM-CB3, TXM-CB12, and SD appeared to be more efficient in inhibiting syncytia formation compared to AD4/NACA, TXM-CB13, or TXM-CB30.

### 3.3. TXM peptides inhibit pseudovirus infection in vitro and in vivo

Next, the compounds were tested for inhibiting pseudovirus infection of ACE2-expressing HEK293 cells (Fig. 4). When pseudoviruses were preincubated with the tested compounds prior to cell infection, TXM-CB3 ( $IC_{50} = 3.11 \pm 0.76$  mM) and TXM-CB30 ( $IC_{50} = 1.30 \pm 0.22$

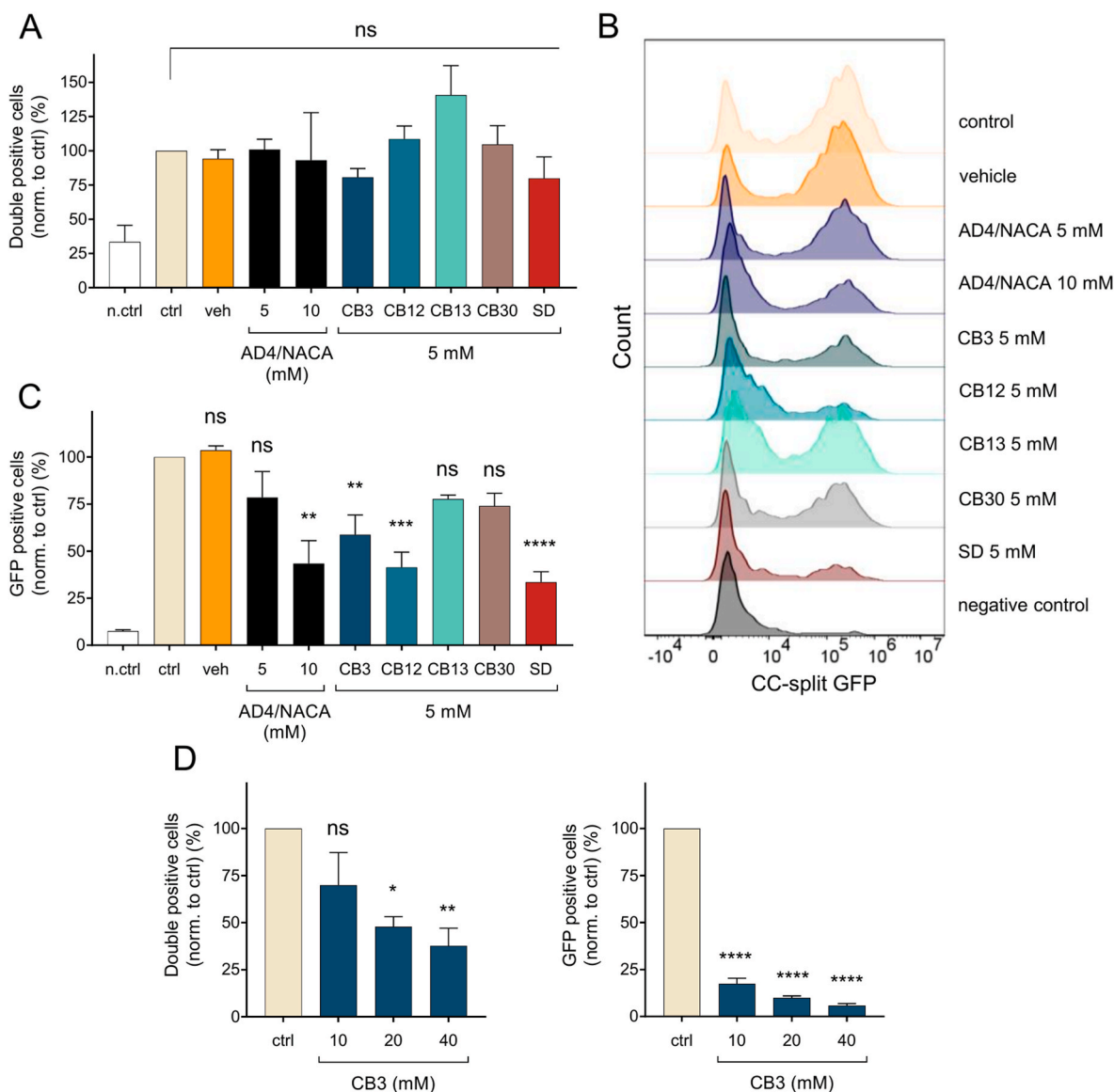


**Fig. 3. Thiol-based peptides inhibit syncytia formation more efficiently than spike-ACE2 interaction.** Cells were transfected with spike, split GFP<sub>(1-10)</sub>:gs:N7 and iRFP<sup>NLS</sup>, or with ACE2, split 3x(N8:g:GFP<sub>11</sub>) and BFP<sup>NLS</sup> plasmids. Spike-expressing cells were preincubated w/o compounds for 30 min and mixed with ACE2-expressing cells for 3 h. Control are untreated cells (ctrl), vehicle are cells treated with peptide solvent (veh). For negative control, cells were transfected with fluorescent dyes only (n.ctrl). Cells were analyzed using flow cytometer. (A) Double-positive iRFP and BFP signal presents cells in interaction and (B, C) GFP positive subgroup presents syncytia forming cells (gating strategy in Suppl. Fig. 3). (D) Cells in interaction together with syncytia forming cells at a higher TXM-CB3 compound concentration. Combined means from 3 indep. exp. (A, C, D) are shown as mean  $\pm$  SEM. Comparison to untreated control (ctrl) was analyzed using one-way ANOVA with Dunnett's multiple comparison test. \*\*\*\*p < 0.0001; \*\*\*p < 0.001; \*\*p < 0.01; \*p < 0.05; non significant (ns). (B) Representatives of three indep. exp. are shown.

mM) appeared to be more effective in inhibiting spike protein pseudotyped viral infection in vitro (Fig. 4B–E) than TXM-CB12 ( $IC_{50} = 6.37 \pm 2.45$  mM), TXM-CB13 ( $IC_{50} = 2.60 \pm 0.60$  mM), and NACA ( $IC_{50} = 12.94 \pm 9.72$  mM). To exclude the possibility of an inhibitory effect due to an intracellular action of TXM peptides, the compounds were preincubated with cells before adding the pseudoviruses. As expected, no significant inhibition of pseudovirus entry was observed (Fig. 4F–G). In addition to SARS-CoV-2, other viruses like HIV, murine leukemia virus, rubella virus, and some other enveloped viruses, are known to express redox-sensitive fusion proteins (reviewed in Fenouillet et al. (2007)). We produced and isolated HIV gp160 protein pseudotyped viruses and tested them with TXM-CB3 ( $IC_{50} = 6.57 \pm 4.60$  mM) and TXM-CB30 ( $IC_{50} = 5.52 \pm 2.51$  mM). As shown, both TXM peptides efficiently and concentration-dependently inhibited HIV gp160 pseudovirus infection in vitro (Fig. 4I). These results indicate a general redox

sensitive mechanistic aspect of viral infection.

The TXM peptides were further tested for preventing spike protein pseudotyped viral infection in vivo. Mice were injected intraperitoneally with TXM-CB3, TXM-CB30, or SD (2 mg/mouse/day) for two consecutive days. On day 2, they were transfected intranasally with DNA plasmids coding for human ACE2 receptor and TMPRSS2, making their respiratory tract susceptible to viral infection. A day later, mice were intranasally infected with spike protein-pseudotyped viruses coding for firefly luciferase. Luciferase expression was detected 24 h later by bioluminescence detection, stating the level of pseudovirus infection. All three TXM peptides exhibited a significant in vivo inhibition of pseudovirus infection (Fig. 5).

In addition, we tested the potential effects of redox structure manipulation of spike protein by TXM peptides on antibody recognition. Antibodies derived from SARS-CoV-2 vaccinated mice still retained the

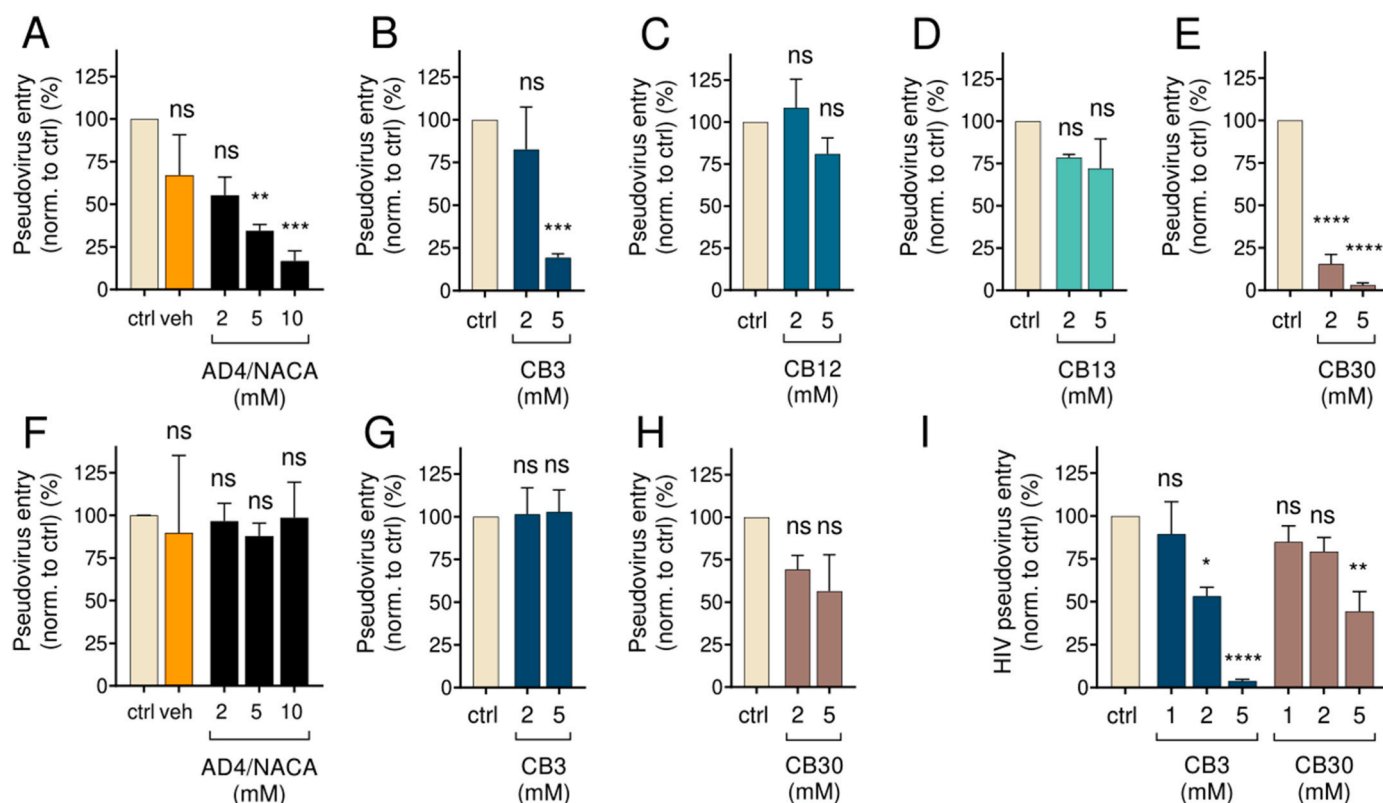


**Fig. 4.** TXM peptides hinder pseudovirus infection of ACE2-expressing cells. (A–H) For the SARS-CoV-2 pseudovirus assay, cells were transfected with ACE2 and *Renilla* luciferase plasmids. (I) For the HIV pseudovirus assay, a stable U87 cell line expressing CD4 and CCR5 receptors was used. (A–E, I) When checked for extracellular activity of TXM peptides, pseudotyped viruses, coding for firefly luciferase, were pre-incubated w/o compounds for 30 min. Control (ctrl) are untreated cells and vehicle (veh) are pseudotyped viruses treated with peptide solvent. (F–H) Possible intracellular effects of TXM peptides on pseudoviral entry were determined by incubating the cells prior to pseudotyped virus infection. In both cases, the day after infection, a (dual) luciferase assay was performed. Combined means from three indep. exp. are shown as mean  $\pm$  SEM. Comparison to untreated infected control (ctrl) was analyzed using one-way ANOVA with Dunnett's multiple comparison test. \*\*\*\* $p < 0.0001$ ; \*\*\* $p < 0.001$ ; \*\* $p < 0.01$ ; \* $p < 0.05$ ; non significant (ns).

ability to recognize TXM treated spike protein, implying that virus surface protein redox changes do not affect conformational epitopes recognized by antibodies until high serum titers ( $1:10^5$ ) (Suppl. Fig. 4). Altogether, these results confirm the efficiency and potential antiviral therapeutic value of TXM peptides.

### 3.4. Thiol-reducing peptides prevent SARS-CoV-2 infection in cells

In addition to inhibiting pseudovirus infection, TXM-CB3 was also tested for an inhibitory effect on the Wuhan, Alpha, Delta, and Omicron variants. The virus was incubated with the TXM-CB3 at the indicated concentrations. After infection, Vero E6 cells were incubated with medium containing the compound. Viral load was determined by RT-qPCR, with GAPDH as a control. When incubated with the virus prior to cell infection, TXM-CB3 efficiently and dose-dependently inhibited cell entry and replication of all tested variants (Wuhan  $IC_{50} = 2.97 \pm 0.38$  mM, Alpha  $IC_{50} = 0.62 \pm 0.22$  mM, Delta  $IC_{50} = 0.94 \pm 0.19$  mM, and Omicron  $IC_{50} = 3.13 \pm 1.06$  mM) (Fig. 6A–D, Suppl. Figs. 5A–D), confirming that targeting conserved motifs is not affected by the different mutations and has broad antiviral applicability of thiolethiol mimetic peptides. The addition of TXM compound after viral infection revealed a limited inhibitory effect on viral replication of Omicron variant ( $IC_{50} = 11.81 \pm 4.90$  mM), further confirming the primary effect of TXM compounds on viral entry (Fig. 6E, Suppl. Fig. 5E).

### 3.5. TXM peptides exert antioxidant/anti-inflammatory activity in vitro

The antioxidative/anti-inflammatory activities of the TXM peptides was determined by monitoring the inhibition of oxidative stress-induced

phosphorylation of the MAPK's ERK1/2 and JNK1/2. PC12 cells were incubated with 5  $\mu$ M auranofin (AuF) for 30 min, washed, and then incubated for an additional 30 min with increasing concentrations of TXM peptide. AuF-induced ERK1/2 or JNK1/2 phosphorylation was reversed in a dose-dependent manner by TXM-CB3 (Fig. 7). Similar activities were previously shown for SD and TXM-CB30 in SH-SY5Y cell line (Wiesen and Atlas, 2022). The efficacy of TXM peptides in reversing MAPK's phosphorylation, was significantly higher compared to AD4/NACA (Bachnoff et al., 2011), consistent with higher potency in inhibiting viral fusion. Despite a comparable in vitro activity, these peptides might have different activity in vivo based on differences in bioavailability, which is governed by membrane permeability, differential proteolysis resistance, and plasma stability.

### 3.6. TXM-peptides mitigate inflammation in vitro and in vivo

Accumulating studies related to infection by SARS-CoV and SARS-CoV-2 have shown high levels of pro-inflammatory cytokines (IFN $\alpha$ , IFN $\gamma$ , IL-1 $\beta$ , IL-6, IL-12, IL-18, IL-33, TNF $\alpha$ , TGF $\beta$ ) and chemokines (CXCL10, CXCL8, CXCL9, CCL2, CCL3, CCL5), which sustain the systemic inflammatory response (Cameron et al., 2008; Channappanavar and Perlman, 2017; Costela-Ruiz et al., 2020; Khalil et al., 2021). The anti-inflammatory effects of TXM peptides were tested using the A549-Dual<sup>TM</sup> cell line where activation of NF- $\kappa$ B and IRF pathway was determined. Cells were stimulated with poly (I:C), a synthetic analog of dsRNA. In cells stimulated by poly (I:C), preincubated with the transfection reagent DOTAP for cytosolic delivery (Fig. 8A), the agonist is recognized by the cytosolic receptors MDA5/RIG-I. When poly (I:C) is added directly to the cell medium (Fig. 8B), it is endocytosed, primarily

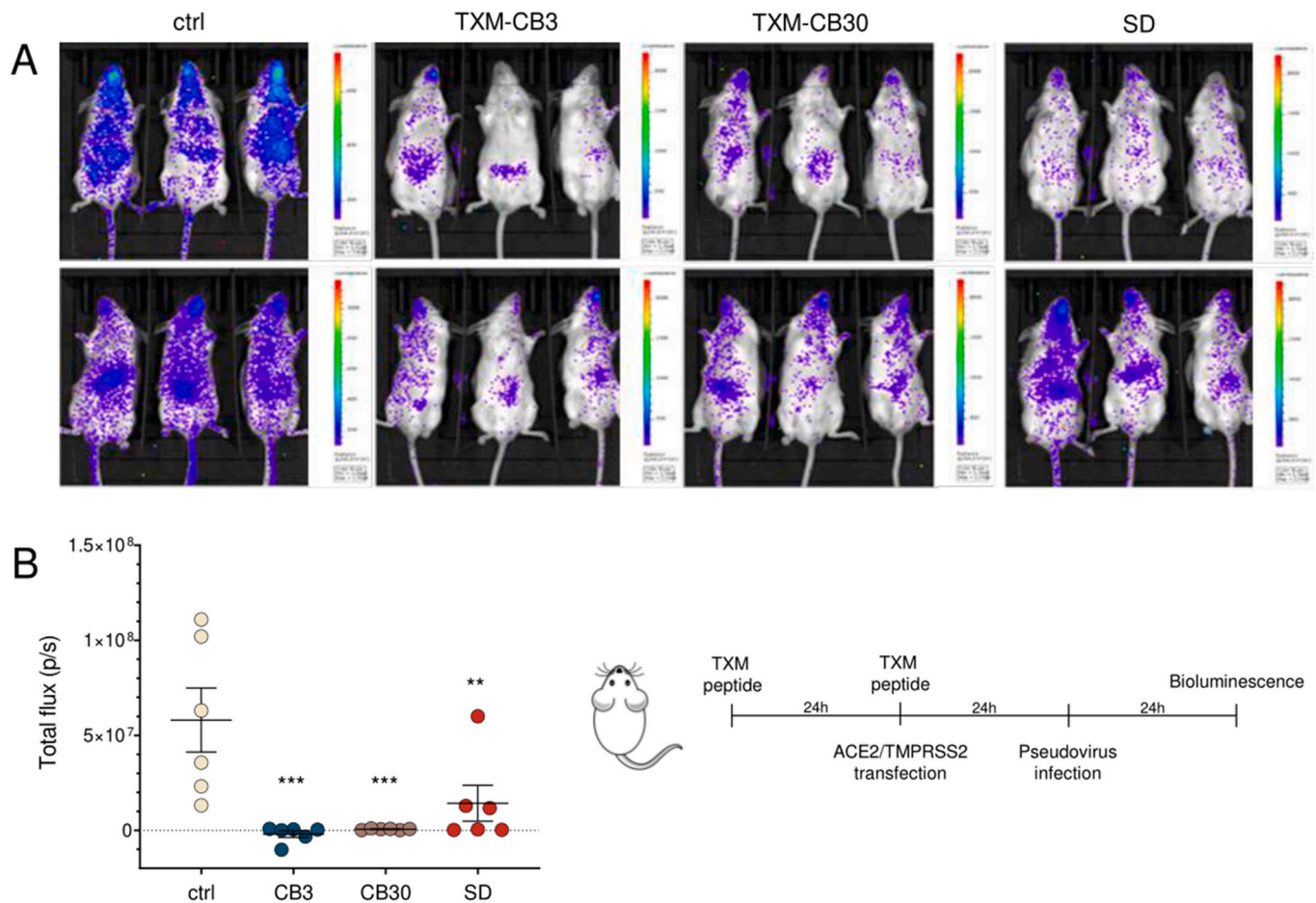


**Fig. 5.** TXM peptides mitigate pseudovirus infection in vivo. Female 10-week old Balb/c mice were i.p. injected with tested compounds for two consecutive days (2 mg/day). On day 2, mice were intranasally transfected with ACE2 receptor and TMPRSS2 plasmids. Animals were infected with spike protein-pseudotyped viruses, coding for firefly luciferase, on day 3, and 24 h postinfection, bioluminescence was measured (presented here as total flux (photons/s)). Comparison to untreated infected control (ctrl) was analyzed using Brown-Forsythe and Welch ANOVA with Dunnett's multiple comparison test. \*\*\* $p < 0.001$ ; \*\* $p < 0.01$ .

triggering TLR3-mediated response (Kawai and Akira, 2008). In both cases, prior activation of inflammatory pathways was mitigated with the addition of TXM-CB30 or AD4/NACA (Fig. 8A and B). Moreover, TXM-CB3 was tested in vivo in LPS-induced inflammation mouse model by determining cell number and cytokines in BAL (Fig. 8C–D, Suppl. Fig. 6). The significant increase in neutrophils and eosinophils induced by LPS in BAL of LPS-treated mice was lowered by TXM-CB3, 47 % and 40 % respectively (Fig. 8C). No significant decrease was observed for B-lymphocytes, T-lymphocytes or macrophages (Suppl. Fig. 6). Cytokine levels were also significantly decreased in BAL of LPS-treated mice, where TXM-CB3 lowered the LPS-induced IL-1 beta, CXCL10, IFN- $\gamma$ , and IL-2 (Fig. 8D).

#### 4. Discussion

The redox state of the cell is regulated mainly by Cys-containing redox-sensitive proteins. Under physiological conditions, most cysteines are non-reactive. However, upon oxidation, thiolate anions with much higher reactivity are formed (Groitl and Jakob, 2014). Under oxidative stress, redox-sensitive viral fusion proteins, including the SARS-CoV-2 spike protein, are present most likely in the oxidized form forming disulfide bonds. During SARS-CoV-2 entry, oxidative state leads to a favorable spike protein binding to the ACE2 receptor, which preserves a structural complementarity between the binding partners (Fossum et al., 2021). Also, other steps in SARS-CoV-2 infection and

pathogenesis (e.g., disturbance of intracellular disulfide-thiol equilibrium) were hypothesized to be linked to oxidative stress (reviewed in Cecchini and Cecchini (2020); Suhail et al. (2020)). Therefore, inhibition of viral binding by disruption of disulfide bonds within the RBD of SARS-CoV-2 spike protein by reestablishing a reducing environment during infection would appear a plausible therapeutic strategy. The importance of Cys residues for RBD function has been previously shown in several ways. The mutation of a single specific Cys residue in RBD did not affect spike-ACE2 interaction but was sufficient to affect spike transition to postfusion conformation necessary for cell fusion process (Manček-Keber et al., 2021). Additionally, thiol-reducing agents, P2119 and P2165, or an exchanger of sulphhydryl groups such as auranofin, appeared to disrupt the pairing of Cys379–Cys432 and Cys391–Cys525 and thereby inhibited cell fusion and viral infection (Manček-Keber et al., 2021; Shi et al., 2022). In the present study, five TXM peptides were tested for inhibition of spike binding to ACE2. All of the peptides appeared to significantly inhibit the interaction, acting at micromolar concentrations with comparable efficiency. The compounds were also able to inhibit spike rearrangements, resulting in inhibition of syncytia formation (in the low millimolar range), which seemed to be more sensitive to reducing agents compared to the spike-ACE2 interaction itself. This observation could be explained by molecular dynamics observations suggesting that all disulfides must be reduced to impair spike binding to ACE2 (Fossum et al., 2021; Hati and Bhattacharyya, 2020), in contrast to a single Cys residue mutation in the RBD that was sufficient

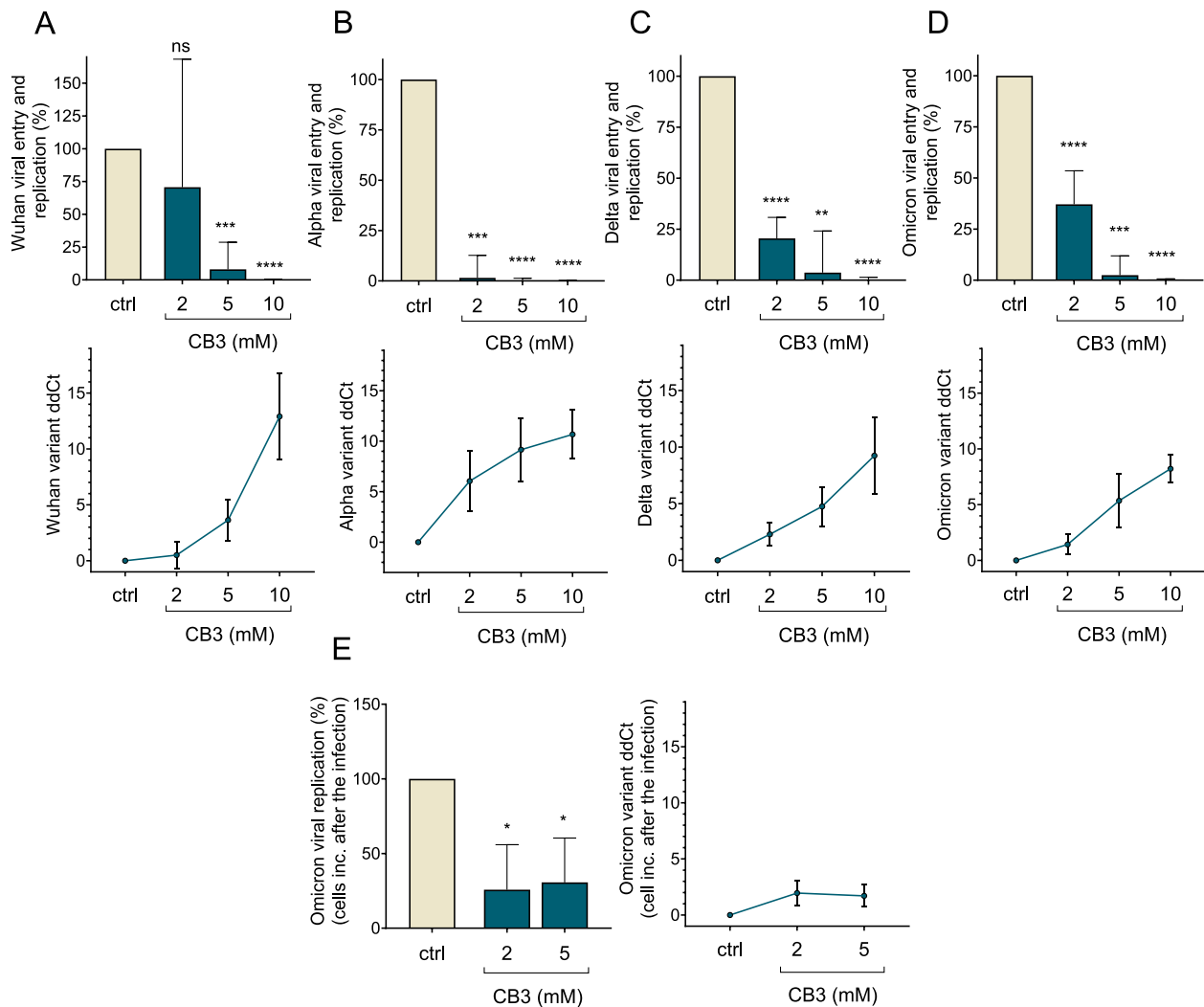


**Fig. 6. TXM-CB3 inhibits viral entry and replication of several SARS-CoV-2 variants.** Wuhan (A), Alpha (B), Delta (C), and Omicron (D) SARS-CoV-2 variants were preincubated for 1 h with TXM-CB3. After 1 h infection of Vero E6 cells, cells were left overnight in a tested compound containing medium. Inhibition of viral replication by TXM peptides was tested by incubating TXM-CB3 with the cells after (E) viral infection. Viral RNA was determined with RT-qPCR targeting the E gene of SARS-CoV-2, using GAPDH as a control. Results are presented as a percentage of viral entry (fold change with corresponding 95 % CI) compared to untreated cells after normalization to GAPDH expression (Brown-Forsythe and Welch ANOVA multiple comparisons test used on  $\Delta$ Ct values). \*\*\*\* $p$  < 0.0001; \*\*\* $p$  < 0.001; \*\* $p$  < 0.01; \* $p$  < 0.05; non significant (ns) with shown  $\Delta\Delta$ Ct values (mean of eight replicates  $\pm$  SD). See also [Suppl. Fig. 5](#).

to mitigate cell fusion (Manček-Keber et al., 2021; Murai et al., 2022).

These observations were confirmed using pseudoviruses, in which only the extracellular part of the virus life cycle participates in receptor binding and cell fusion. A significant inhibition of pseudovirus infection was exhibited by TXM peptides in vitro and was confirmed in vivo in a mouse model of pseudoviral infection. The TXM-CB3, TXM-CB30, and SD peptides significantly inhibited spike protein pseudotyped viral infection in a preventive manner, confirming their potential antiviral activity. Moreover, we also demonstrated an inhibitory effect of TXM peptide on cell entry of SARS-CoV-2 Wuhan, Alpha, Delta, and Omicron variants. We observed minimal impact of TXM peptide on viral replication, which can not be explained solely by a direct effect of TXM peptide on proteins involved in replication because a combination of antioxidant activity and attenuation of SARS-CoV-2-triggered cytokine storm may inhibit viral replication as well as proposed by Citi et al. (2020). Due to the different replication kinetics and infectivity of SARS-CoV-2 variants in cell culture models (Mautner et al., 2022), the exact inhibitory efficiency among the different strains could not be determined. Nonetheless, viral infection by all variants appeared to be inhibited by TXM-CB3 in a dose-dependent manner, further confirming

the TXM peptides' viral inhibitory activity.

Manipulation of the native disulfide network has been shown to be beneficial also for viral envelope glycoproteins. Specific thiol/disulfide rearrangements of viral envelope proteins are required for efficient incorporation of fusion peptides into the cell surface (reviewed in Fenouillet et al. (2007)). For example, HIV fusion has been shown to be blocked either by inhibition of gp120 receptor binding following mild chemical reduction or by inhibiting protein disulfide isomerase (PDI) on the cell surface, using free sulfhydryl reagents and non-permeant inhibitors of PDI. This approach has been proposed for anti-HIV therapy due to the low probability of resistance development (Fenouillet et al., 2007). Herein, we demonstrated that TXM peptides could also prevent HIV gp160 protein pseudotyped viral entry into cells, implying a broad spectrum of antiviral activity.

COVID-19 patients have significantly lower plasma levels of vitamins C, A, and E and a lower activity of glutathione peroxidase and superoxide dismutase. In addition, they display lower levels of minerals like selenium, magnesium, or copper, which comprise antioxidant, anti-inflammatory, immunomodulatory, and antiviral potential for antioxidant compounds (Pisoschi et al., 2022; Žarković et al., 2022).

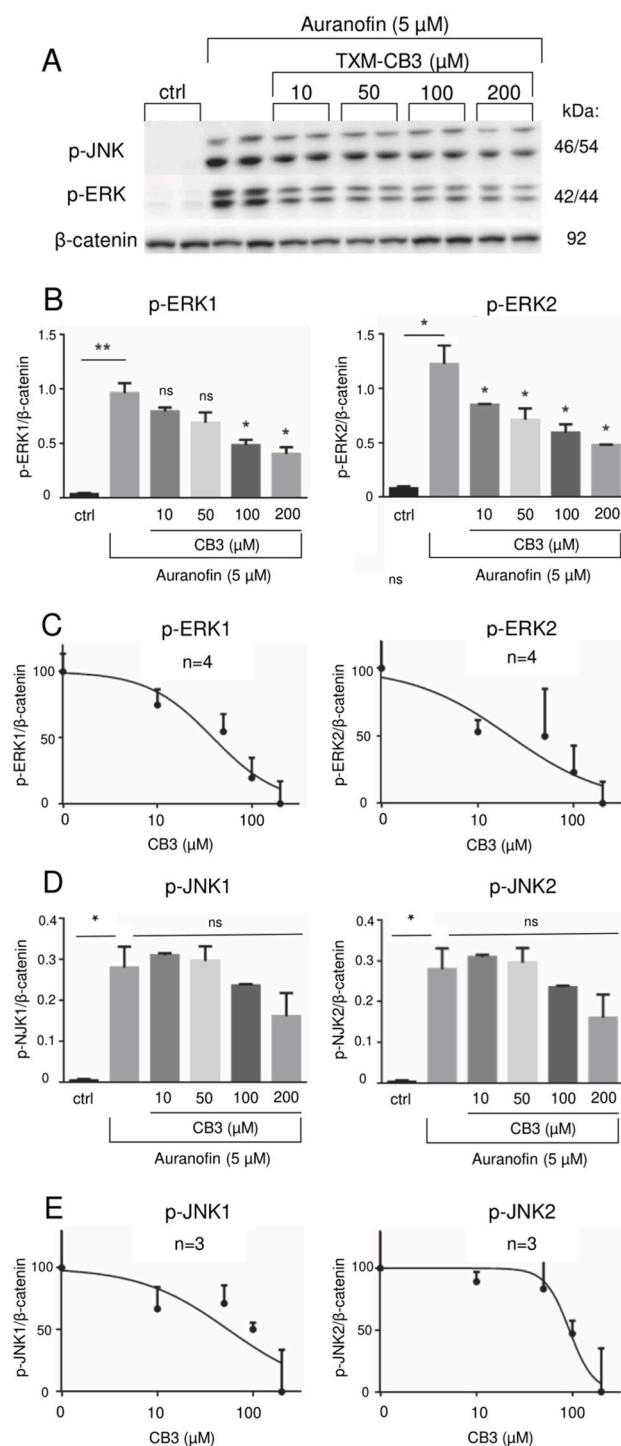


**Fig. 7. TXM-CB3 reverses auranofin-induced phosphorylation of ERK1/2 and JNK1/2 in PC12 cells.** (A) PC12 cells were incubated with 5 μM auranofin for 30 min, washed, and treated w/o TXM-CB3. Equal amounts of total proteins were loaded on SDS-PAGE and analyzed by immunoblotting using the corresponding ERK1/2 and JNK1/2 antibodies. The ratios of phosphorylated ERK1/2 and JNK1/2 to the β-catenin were calculated. (B, C) The values shown for pERK1 and pERK2 and (D, E) for pJNK1 and pJNK 2 are averages (±SEM) based on 3 indep. exp., normalized to the phosphorylation state of cells treated with auranofin and plotted with a linear regression program. For statistical analysis, Student's *t*-test (two populations) was used. \**p* < 0.05; \*\**p* < 0.01; non significant (ns).

Correspondingly, COVID-19 survivors have a significantly higher H<sub>2</sub>S level compared to considerably higher mortality among patients with lower H<sub>2</sub>S levels (Dai et al., 2021). Some clinical observations reported improved medical conditions of patients with COVID-19 using vitamin C (reviewed by Milani et al. (2021)), which inhibited spike fusion using the same mechanism (Manček-Keber et al., 2021). Also, N-acetyl cysteine (NAC), which is a potential H<sub>2</sub>S-releasing donor, improved symptoms of severe COVID-19 when administered i.v. (Ibrahim et al., 2020). The thiol compound cysteamine decreased neutrophilic lung inflammation and alveolar hemorrhage in SARS-CoV-2 infected hamsters (Khanna et al., 2022). NAC and cysteamine are both FDA-approved medicinal thiols, and along with other compounds, e.g., amifostine and captopril, they are used for different clinical states, such as N-acetyl-p-aminophenol overdose, radioprotection, hypertension (reviewed in Pfaff et al. (2020)), without serious side effects. The short retention time of TXM peptides in the blood due to membrane permeability, as discussed further, and a minimal effect on conformational epitopes, strongly suggest that they do not participate in antibody-dependent enhancement (ADE). Since ADE contributes to enhanced viral infection, its evaluation plays an important role in novel vaccines and therapeutic developments. Although ADE in the context of SARS-CoV-2 has been a concern, the evidence of significant ADE is limited. Despite a clear evidence that antibodies against the original viruses have reduced neutralization capacity against mutant strains, there is a lack of robust data for a clear ADE effect (Nakayama and Shioda, 2023; Yang and Xu, 2022).

The TXM peptides were designed to include two Cys residues flanking either two amino acids (-Cys-X-X-Cys-) or a single amino acid residue (-Cys-X-Cys-) with acetylated N-terminus and amidated C-terminus to facilitate membrane permeability and intracellular targeting (Atlas, 2021; Bachnoff et al., 2011; Cohen-Kutner et al., 2013). This motif is present in thioredoxin and glutaredoxin and is responsible for most of the oxido/reductase modifications within the cells (Holmgren, 1968; Lundström and Holmgren, 1993; Groitl and Jakob, 2014). In vivo, the biological activity of the TXM peptides depends on subcellular localization, free-thiol stability, and the Cys neighboring amino acid residues (Holmgren, 1968; Lundström and Holmgren, 1993). Upon cell entry, TXM peptides are cleaved by intracellular proteases, producing a cluster of different Cys-containing proteolytic fragments. Each fragment containing a Cys residue can serve as a redox-active reagent, a metal chelator, a ROS scavenger, and a GSH precursor. The cluster of multiple Cys-containing fragments generated by each TXM peptide represents a redox "cluster bomb" (Atlas, 2021), making them long-lasting potent antioxidants and anti-inflammatory reagents, both in vitro and in vivo (Bachnoff et al., 2011; Canesi et al., 2019; Cohen-Kutner et al., 2013; Hemling et al., 2020; Kim et al., 2011; Lejnev et al., 2016). In accordance, TXM-CB30 efficiently mitigated ongoing viral inflammation in lung cells stimulated with dsRNA. Also, the significant decrease in the number of neutrophils and eosinophils, IL-1 beta, IFN-γ, CXCL10/IP, and IL-2 in BAL fluid demonstrated in the LPS-induced inflammation mouse model subsequent to i.v. injection of TXM-CB3 further confirmed the TXM peptides' dual antioxidant/anti-inflammatory activities and their potential role in reversing cytokine/inflammatory consequences.

The latest 2023 surge in COVID-19 cases is not surprising since the infection cycle is expected to occur every six months now that all COVID-19 restrictions have been removed. Along with repeated infections, there is also the risk of new viral strains to outcompete with circulating variants in terms of transmissibility and severity. Highly infectious variants such as XBB currently dominate, while immunity is waning even in highly vaccinated or previously infected populations (Ye, 2023). Humoral immunity generated against Omicron variants BA.5 and BF.7, for example, offers about four months of protection against strains such as XBB (Chen et al., 2023). A cohort study showed that reinfections add to the risk of death, hospitalization, and sequelae in multiple organ systems (Bowe et al., 2022). Interestingly, recent reports have demonstrated neurological effects of mild COVID-19 in animal

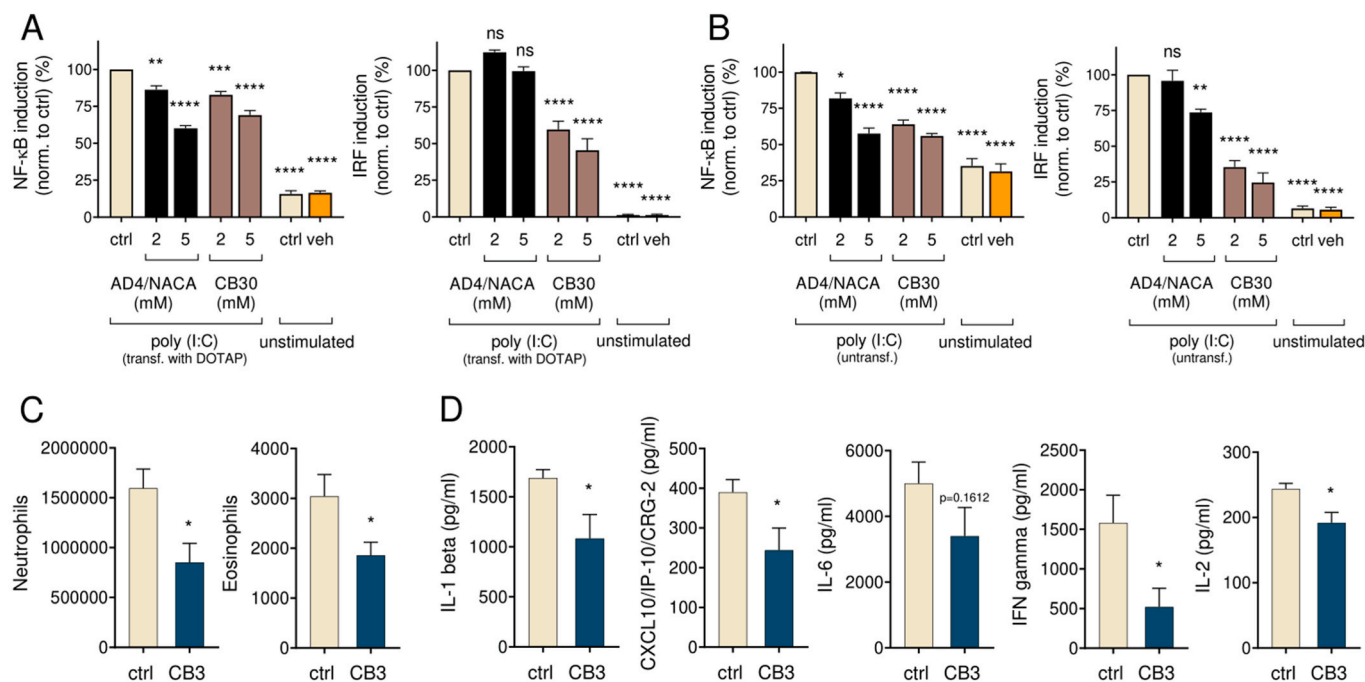


**Fig. 8. TXM peptides lower dsRNA and LPS induced inflammation.** (A, B) Anti-inflammatory effects of TXM-CB30 were tested using poly (I:C) stimulation of cytosolic MDA5/RIG-I (with DOTAP as transfection reagent) (A) or endosomal TLR3 (stimulant added to cell medium) (B) receptors in A549-Dual™ cell line. Three hours after stimulation cells were treated w/o compounds. The next day, NF-κB (by measuring SEAP) and IRF (by measuring *Luciferase* pathway activation) were determined. Control are untreated cells (ctrl), vehicle are cells treated with peptide solvent (veh). (C, D) LPS-challenged mice were injected i.v. with TXM-CB3 at 3 time points: 15 min prior to LPS, 24 h and 48 h after LPS. Mice were sacrificed 72 h after the LPS challenge. (C) The number of neutrophils and eosinophils in BAL fluid of LPS (ctrl) and LPS-TXM-CB3 treated mice (CB3) was determined using flow cytometer. (D) Levels of IL-1 beta, CXCL10, IFN-γ, IL-2 in BAL fluid of LPS (ctrl) and TXM-CB3 treated LPS-mice (CB3) were determined using ELISA. For statistical analysis, one-way ANOVA with Dunnett's multiple comparison test or Student's *t*-test (two populations, Welch's correction applied when appropriate) were used. \*\*\*\**p* < 0.0001; \*\**p* < 0.01; \**p* < 0.05; non significant (ns). See also [Suppl. Fig. 6](#).

model (Fernández-Castañeda et al., 2022). Therefore, the brain-protecting activity of TXM peptides that was previously shown in mild brain injury (mTBI) and high-glucose disorders (Baratz-Goldstein et al., 2016; Cohen-Kutner et al., 2013; Lejnev et al., 2016; Hemling et al., 2020) might be effective also in alleviating neurological long-COVID-19 symptoms.

## 5. Conclusions

*In summary*, in the present study, we confirm the importance of antioxidant/anti-inflammatory activities in inhibiting viral infection and highlight the therapeutic potential of TXM peptides in preventing and treating SARS-CoV-2 infection and its consequences. Our results show that the TXM peptides appear to modify the fusion reaction of several viral fusion proteins, acting as antioxidants and anti-inflammatory reagents. These results suggest that TXM peptides may be a beneficial treatment to prevent viral infections and syncytia formation combined with reducing the release of inflammatory cytokines.

## CRedit authorship contribution statement

**Tea Govednik:** Writing – original draft, Investigation, Formal analysis, Data curation. **Duško Lainsček:** Investigation. **Urška Kuhar:** Methodology. **Marva Lachish:** Investigation. **Sandra Janežič:** Resources. **Malan Štrbenc:** Investigation. **Uroš Krapež:** Methodology. **Roman Jerala:** Writing – review & editing, Funding acquisition, Conceptualization. **Daphne Atlas:** Writing – original draft, Funding acquisition, Formal analysis, Conceptualization. **Mateja Manček-Keber:** Writing – original draft, Supervision, Methodology, Conceptualization.

## Declaration of competing interest

The authors declare that they have no known competing financial interests or personal relationships that could have appeared to influence the work reported in this paper.

## Data availability

Data will be made available on request.

## Acknowledgements

This study was financially supported by the Slovenian Research and Innovation Agency (project no. V4-2038, research core no. P4-0176, P4-0092, and P4-0053), Virofight project (H2020-FETOPEN-2018-2019-2020-01) and »Yissum«, The Hebrew University Tech Transfer Company. We thank Bruno Correia from EPFL for recombinant spike protein, Mojca Benčina for technical support, Igor Locatelli for help with statistical analysis, as well as Patricia Tandara and Brigita Slavec for laboratory work on in vitro cell infection experiments.

## Appendix A. Supplementary data

Supplementary data to this article can be found online at <https://doi.org/10.1016/j.antiviral.2024.105806>.

## References

Anthony, R.P., Paredes, A.M., Brown, D.T., 1992. Disulfide bonds are essential for the stability of the Sindbis virus envelope. *Virology* 190, 330–336. [https://doi.org/10.1016/0042-6822\(92\)91219-K](https://doi.org/10.1016/0042-6822(92)91219-K).

- Atlas, D., 2021. Emerging therapeutic opportunities of novel thiol-amides, NAC-amide (AD4/NACA) and thioredoxin mimetics (TXM-Peptides) for neurodegenerative-related disorders. *Free Radic. Biol. Med.* 176, 120–141. <https://doi.org/10.1016/j.freeradbiomed.2021.08.239>.
- Bachnoff, N., Trus, M., Atlas, D., 2011. Alleviation of oxidative stress by potent and selective thioredoxin-mimetic peptides. *Free Radic. Biol. Med.* 50, 1355–1367. <https://doi.org/10.1016/j.freeradbiomed.2011.02.026>.
- Baratz-Goldstein, R., Deselms, H., Heim, L.R., Khomski, L., Hoffer, B.J., Atlas, D., Pick, C. G., 2016. Thioredoxin-mimetic-peptides protect cognitive function after mild traumatic brain injury (mTBI). *PLoS One* 11, e0157064. <https://doi.org/10.1371/JOURNAL.PONE.0157064>.
- Barbouche, R., Miquelis, R., Jones, I.M., Fenouillet, E., 2003. Protein-disulfide isomerase-mediated reduction of two disulfide bonds of HIV envelope glycoprotein 120 occurs post-CXCR4 binding and is required for fusion. *J. Biol. Chem.* 278, 3131–3136. <https://doi.org/10.1074/jbc.M205467200>.
- Bartov, O., Sultana, R., Butterfield, D.A., Atlas, D., 2006. Low molecular weight thiol amides attenuate MAPK activity and protect primary neurons from A $\beta$ (1–42) toxicity. *Brain Res.* 1069, 198–206. <https://doi.org/10.1016/j.brainres.2005.10.079>.
- Bowe, B., Xie, Y., Al-Aly, Z., 2022. Acute and postacute sequelae associated with SARS-CoV-2 reinfection. *Nat. Med.* 28, 2398–2405. <https://doi.org/10.1038/s41591-022-02051-3>.
- Bussani, R., Schneider, E., Zentilin, L., Collesi, C., Ali, H., Braga, L., Concetta, M., Colliva, A., Zanonati, F., Berlot, G., Silvestri, F., Zacchigna, S., Giacca, M., 2020. EBioMedicine Persistence of viral RNA , pneumocyte syncytia and thrombosis are hallmarks of advanced COVID-19. *Pathology* 61. <https://doi.org/10.1016/j.ebiom.2020.103104>.
- Cameron, M.J., Bermejo-Martin, J.F., Danesh, A., Muller, M.P., Kelvin, D.J., 2008. Human immunopathogenesis of severe acute respiratory syndrome (SARS). *Virus Res.* 133, 13–19. <https://doi.org/10.1016/j.VIRUSRES.2007.02.014>.
- Canesi, F., Mateo, V., Couchie, D., Karabina, S., Nègre-Salvayre, A., Rouis, M., El Hadri, K., 2019. A thioredoxin-mimetic peptide exerts potent anti-inflammatory, antioxidant, and atheroprotective effects in ApoE2.Ki mice fed high fat diet. *Cardiovasc. Res.* 115, 292–301. <https://doi.org/10.1093/CVR/CVY183>.
- Cecchini, R., Cecchini, A.L., 2020. SARS-CoV-2 infection pathogenesis is related to oxidative stress as a response to aggression. *Med. Hypotheses* 143, 110102. <https://doi.org/10.1016/J.MEHY.2020.110102>.
- Channappanavar, R., Perlman, S., 2017. Pathogenic human coronavirus infections: causes and consequences of cytokine storm and immunopathology. *Semin. Immunopathol.* 39 (5), 529–539. <https://doi.org/10.1007/S00281-017-0629-X>, 2017 39.
- Chen, X., Xu, Y., Xie, Y., Song, W., Hu, Y., Yisimayi, A., Yang, S., Shao, F., Geng, L., Wang, Y., Gao, H., Shi, Y., Zhang, S., Jin, R., Shen, Z., Cao, Y., 2023. Protective effect of plasma neutralization from prior SARS-CoV-2 Omicron infection against BA.5 subvariant symptomatic reinfection. *Lancet Reg Health West Pac* 33, 100758. <https://doi.org/10.1016/j.lanwpc.2023.100758>.
- Citi, V., Martelli, A., Brancalione, V., Brogi, S., Gojón, G., Montanaro, R., Morales, G., Testai, L., Calderone, V., 2020. Anti-inflammatory and antiviral roles of hydrogen sulfide: rationale for considering H2S donors in COVID-19 therapy. *Br. J. Pharmacol.* 177, 4931–4941. <https://doi.org/10.1111/bph.15230>.
- Cohen-Kutner, M., Khomsky, L., Trus, M., Aisner, Y., Niv, M.Y., Benhar, M., Atlas, D., 2013. Thioredoxin-mimetic peptides (TXM) reverse auranofin induced apoptosis and restore insulin secretion in insulinoma cells. *Biochem. Pharmacol.* 85, 977–990. <https://doi.org/10.1016/j.bcp.2013.01.003>.
- Corman, V.M., Landt, O., Kaiser, M., Molenkamp, R., Meijer, A., Chu, D.K.W., Bleicker, T., Brünink, S., Schneider, J., Schmidt, M.L., Mulders, D.G.J.C., Haagmans, B.L., Van Der Veer, B., Van Den Brink, S., Wijsman, L., Goderski, G., Romette, J.L., Ellis, J., Zambon, M., Peiris, M., Goossens, H., Reusken, C., Koopmans, M.P.G., Drosten, C., 2020. Detection of 2019 novel coronavirus (2019-nCoV) by real-time RT-PCR. *Euro Surveill.* 25. <https://doi.org/10.2807/1560-7917.ES.2020.25.3.2000045>.
- Costela-Ruiz, V.J., Illescas-Montes, R., Puerta-Puerta, J.M., Ruiz, C., Melguizo-Rodríguez, L., 2020. SARS-CoV-2 infection: the role of cytokines in COVID-19 disease. *Cytokine Growth Factor Rev.* <https://doi.org/10.1016/j.cytogr.2020.06.001>.
- Dai, J., Teng, X., Jin, S., Wu, Y., 2021. The antiviral roles of hydrogen sulfide by blocking the interaction between SARS-CoV-2 and its potential cell surface receptors. *Oxid. Med. Cell. Longev.* 2021. <https://doi.org/10.1155/2021/7866992>.
- Fenouillet, E., Barbouche, R., Jones, I.M., 2007. Cell entry by enveloped viruses: redox considerations for HIV and SARS-coronavirus. *Antioxidants Redox Signal.* <https://doi.org/10.1089/ars.2007.1639>.
- Fernández-Castañeda, A., Lu, P., Geraghty, A.C., Song, E., Lee, M.-H., Wood, J., O’Dea, M.R., Dutton, S., Shamardani, K., Nwangwu, K., Mancusi, R., Yalcın, B., Taylor, K.R., Acosta-Alvarez, L., Malacon, K., Keough, M.B., Ni, L., Woo, P.J., Contreras-Esquivel, D., Toland, A.M.S., Gehlhausen, J.R., Klein, J., Takahashi, T., Silva, J., Israelow, B., Lucas, C., Mao, T., Peña-Hernández, M.A., Tabachnikova, A., Homer, R.J., Tabacof, L., Tosto-Mancuso, J., Breyman, E., Kontorovich, A., McCarthy, D., Quezado, M., Vogel, H., Hefti, M.M., Perl, D.P., Liddelow, S., Folkerth, R., Putrino, D., Nath, A., Iwasaki, A., Monje, M., 2022. Mild respiratory COVID can cause multi-lineage neural cell and myelin dysregulation. *Cell.* <https://doi.org/10.1016/j.cell.2022.06.008>.
- Fossum, C.J., Laatsch, B.F., Lowater, H.R., Narkiewicz-Jodko, A.W., Lonzarich, L., Hati, S., Bhattacharyya, S., 2021. Pre-existing oxidative stress creates a docking-ready conformation of the SARS-CoV-2 receptor-binding domain. *Cite This: ACS Bio Med Chem Au* 2022, 93. <https://doi.org/10.1021/acsbiochemchem.1c00040>.
- Fraternal, A., De Angelis, M., De Santis, R., Amatore, D., Masini, S., Monitola, F., Menotta, M., Bianucci, F., Bartocchini, F., Retini, M., Fiori, V., Fioravanti, R., Magurano, F., Chiarantini, L., Lista, R.F., Piersanti, G., Palamara, A.T., Nencioni, L., Magnani, M., Crinelli, R., 2023. Targeting SARS-CoV-2 by synthetic dual-acting thiol compounds that inhibit Spike/ACE2 interaction and viral protein production. *Faseb. J.* 37, e22741. <https://doi.org/10.1096/fj.202201157RR>.
- Grinberg, L., Fibach, E., Amer, J., Atlas, D., 2005. N-acetylcysteine amide, a novel cell-permeating thiol, restores cellular glutathione and protects human red blood cells from oxidative stress. *Free Radic. Biol. Med.* 38, 136–145. <https://doi.org/10.1016/j.freeradbiomed.2004.09.025>.
- Grishin, A.M., Dolgova, N.V., Landreth, S., Fiset, O., Pickering, I.J., George, G.N., Falzarano, D., Cygler, M., 2022. Disulfide bonds play a critical role in the structure and function of the receptor-binding domain of the SARS-CoV-2 spike antigen. *J. Mol. Biol.* 434, 167357. <https://doi.org/10.1016/j.jmb.2021.167357>.
- Groitt, B., Jakob, U., 2014. Thiol-based redox switches. *Biochim. Biophys. Acta, Proteomics* 1844, 1335–1343. <https://doi.org/10.1016/j.bbapap.2014.03.007>.
- Gros, C., Linder, M., Wengler, Gisela, Wengler, Gerd, 1997. Analyses of disulfides present in the rubella virus E1 glycoprotein. *Virology* 230, 179–186. <https://doi.org/10.1006/VIRO.1997.8462>.
- Hati, S., Bhattacharyya, S., 2020. Impact of thiol-disulfide balance on the binding of covid-19 spike protein with angiotensin-converting enzyme 2 receptor. *ACS Omega* 5, 16292–16298. <https://doi.org/10.1021/acscomega.0c02125>.
- Hemling, P., Zibrova, D., Strutz, J., Sohrabi, Y., Desoye, G., Schulten, H., Findeisen, H., Heller, R., Godfrey, R., Waltenberger, J., 2020. Hyperglycemia-induced endothelial dysfunction is alleviated by thioredoxin mimetic peptides through the restoration of VEGFR-2-induced responses and improved cell survival. *Int. J. Cardiol.* 308, 73–81. <https://doi.org/10.1016/j.ijcard.2019.12.065>.
- Holmgren, A., 1968. Thioredoxin. 6. The amino acid sequence of the protein from *Escherichia coli* B. *Eur. J. Biochem.* 6, 475–484. <https://doi.org/10.1111/J.1432-1033.1968.TB00470.X>.
- Huang, Y., Yang, C., Xu, X., Feng, X., Xu, W., Liu, S., wen, 2020. Structural and functional properties of SARS-CoV-2 spike protein: potential antiviral drug development for COVID-19. *Acta Pharmacol. Sin.* 41, 1141–1149. <https://doi.org/10.1038/s41401-020-0485-4>.
- Ibrahim, H., Perl, A., Smith, D., Lewis, T., Kon, Z., Goldenberg, R., Yarta, K., Staniloae, C., Williams, M., 2020. Therapeutic blockade of inflammation in severe COVID-19 infection with intravenous N-acetylcysteine. *Clin. Immunol.* 219, 293. <https://doi.org/10.1016/j.clim.2020.108544>.
- Janežic, S., Mahnic, A., Kuhar, U., Kovač, J., Jenko Bizjan, B., Koritnik, T., Tesovnik, T., Šket, R., Krapež, U., Slavec, B., Malovrh, T., Battelino, T., Rupnik, M., Zohar Cretnik, T., 2023. SARS-CoV-2 molecular epidemiology in Slovenia, January to September 2021. *Euro Surveill.* 28, 2200451. <https://doi.org/10.2807/1560-7917.ES.2023.28.8.2200451>.
- Kawai, T., Akira, S., 2008. Toll-like receptor and RIG-1-like receptor signaling. *Ann. N. Y. Acad. Sci.* 1143, 1–20. <https://doi.org/10.1196/ANNALS.1443.020>.
- Khalil, B.A., Elemam, N.M., Maghazachi, A.A., 2021. Chemokines and chemokine receptors during COVID-19 infection. *Comput. Struct. Biotechnol. J.* <https://doi.org/10.1016/j.csbj.2021.01.034>.
- Khanna, K., Raymond, W., Jin, J., Charbit, A.R., Gitlin, I., Tang, M., Werts, A.D., Barrett, E.G., Cox, J.M., Birch, S.M., Martinelli, R., Sperber, H.S., Franz, S., Pillai, S., Healy, A.M., Duff, T., Oscarson, S., Hoffmann, M., Pöhlmann, S., Simmons, G., Fahy, J.V., 2021. Thiol drugs decrease SARS-CoV-2 lung injury in vivo and disrupt SARS-CoV-2 spike complex binding to ACE2 in vitro. *bioRxiv* 12 (8), 415505. <https://doi.org/10.1101/2020.12.08.415505>, 2020.
- Khanna, K., Raymond, W.W., Jin, J., Charbit, A.R., Gitlin, I., Tang, M., Werts, A.D., Barrett, E.G., Cox, J.M., Birch, S.M., Martinelli, R., Sperber, H.S., Franz, S., Duff, T., Hoffmann, M., Healy, A.M., Oscarson, S., Pöhlmann, S., Pillai, S.K., Simmons, G., Fahy, J.V., 2022. Exploring antiviral and anti-inflammatory effects of thiol drugs in COVID-19. *Am. J. Physiol. Lung Cell Mol. Physiol.* 323, L372–L389. <https://doi.org/10.1152/ajplung.00136.2022>.
- Kim, S.R., Lee, K.S., Park, S.J., Min, K.H., Lee, M.H., Lee, K.A., Bartov, O., Atlas, D., Lee, Y.C., 2011. A novel dithiol amide CEB3 attenuates allergic airway disease through negative regulation of p38 mitogen-activated protein kinase. *Am. J. Respir. Crit. Care Med.* 183, 1015–1024. <https://doi.org/10.1164/rccm.200906-0902OC>.
- Krey, T., Thiel, H.-J., Rümener, T., 2005. Acid-resistant bovine pestivirus requires activation for pH-triggered fusion during entry. *J. Virol.* 79, 4191–4200. <https://doi.org/10.1128/JVI.79.7.4191-4200.2005>.
- Lainšček, D., Fink, T., Forstnerič, V., Hafner-Bratkovič, I., Orehek, S., Strmšek, Ž., Manček-Keber, M., Pečan, P., Esih, H., Malenšek, Š., Aupič, J., Dekleva, P., Plaper, T., Vidmar, S., Kadunc, L., Benčina, M., Omersa, N., Anderluh, G., Pojfer, F., Lau, K., Hacker, D., Correia, B.E., Peterhoff, D., Wagner, R., Bergant, V., Herrmann, A., Pichlmair, A., Jerala, R., 2021. A nanoscaffolded spike-rbd vaccine provides protection against sars-cov-2 with minimal anti-scaffold response. *Vaccines* 9, 1–21. <https://doi.org/10.3390/vaccines9050431>.
- Lan, J., Ge, J., Yu, J., Shan, S., Zhou, H., Fan, S., Zhang, Q., Shi, X., Wang, Q., Zhang, L., Wang, X., 2020. Structure of the SARS-CoV-2 spike receptor-binding domain bound to the ACE2 receptor. *Nature* 581, 215–220. <https://doi.org/10.1038/s41586-020-2180-5>.
- Lejnev, K., Khomsky, L., Bokvist, K., Mistrjel-Zarbib, S., Naveh, T., Farb, T.B., Alsiná-Fernández, J., Atlas, D., 2016. Thioredoxin-mimetic peptides (TXM) inhibit inflammatory pathways associated with high-glucose and oxidative stress. *Free Radic. Biol. Med.* 99, 557–571. <https://doi.org/10.1016/j.freeradbiomed.2016.09.011>.
- Livak, K.J., Schmittgen, T.D., 2001. Analysis of relative gene expression data using real-time quantitative PCR and the 2 $^{-\Delta\Delta CT}$  method. *Methods* 25, 402–408. <https://doi.org/10.1006/meth.2001.1262>.
- Lundström, J., Holmgren, A., 1993. Determination of the reduction—oxidation potential of the thioredoxin-like domains of protein disulfide-isomerase from the equine

- with glutathione and thioredoxin. *Biochemistry* 32, 6649–6655. <https://doi.org/10.1021/bi00077a018>.
- Manček-Keber, M., Hafner-Bratkovič, I., Lainšček, D., Benčina, M., Govednik, T., Orehek, S., Plaper, T., Jazbec, V., Bergant, V., Grass, V., Pichlmair, A., Jerala, R., 2021. Disruption of disulfides within RBD of SARS-CoV-2 spike protein prevents fusion and represents a target for viral entry inhibition by registered drugs. *FASEB (Fed. Am. Soc. Exp. Biol.) J.* 35, 1–14. <https://doi.org/10.1096/fj.202100560R>.
- Mautner, L., Hoyos, M., Dangel, A., Berger, C., Ehrhardt, A., Baiker, A., 2022. Replication kinetics and infectivity of SARS-CoV-2 variants of concern in common cell culture models. *Virology* 19 <https://doi.org/10.1186/s12985-022-01802-5>.
- Meng, B., Abdullahi, A., Ferreira, I.A.T.M., Goonawardane, N., Saito, A., Kimura, I., Yamasoba, D., Gerber, P.P., Fathi, S., Rathore, S., Zepeda, S.K., Papa, G., Kemp, S.A., Ikeda, T., Toyoda, M., Tan, T.S., Kuramochi, J., Mitsunaga, S., Ueno, T., Shirakawa, K., Takaori-Kondo, A., Brevini, T., Mallery, D.L., Charles, O.J., Bowen, J. E., Joshi, A., Walls, A.C., Jackson, L., Martin, D., Smith, K.G.C., Bradley, J., Briggs, J. A.G., Choi, J., Madisson, E., Meyer, K.B., Mlcochova, P., Ceron-Gutierrez, L., Doffinger, R., Teichmann, S.A., Fisher, A.J., Pizzuto, M.S., de Marco, A., Corti, D., Hosmillo, M., Lee, J.H., James, L.C., Thukral, L., Veessler, D., Sigal, A., Sampaziotis, F., Goodfellow, I.G., Matheson, N.J., Sato, K., Gupta, R.K., 2022. Altered TMPRSS2 usage by SARS-CoV-2 Omicron impacts infectivity and fusogenicity. *Nature* 603, 706–714. <https://doi.org/10.1038/s41586-022-04474-x>.
- Milani, G.P., Macchi, M., Guz-Mark, A., 2021. Vitamin C in the treatment of COVID-19. *Nutrients* 13. <https://doi.org/10.3390/NU13041172>.
- Murae, M., Shimizu, Y., Yamamoto, Y., Kobayashi, A., Hourai, M., Inoue, T., Irie, T., Gamba, R., Kondo, Y., Nakano, Y., Miyazaki, S., Yamada, D., Saitoh, A., Ishii, I., Onodera, T., Takahashi, Y., Wakita, T., Fukasawa, M., Noguchi, K., 2022. The function of SARS-CoV-2 spike protein is impaired by disulfide-bond disruption with mutation at cysteine-488 and by thiol-reactive N-acetyl-cysteine and glutathione. *Biochem. Biophys. Res. Commun.* 597, 30–36. <https://doi.org/10.1016/j.bbrc.2022.01.106>.
- Nakayama, E.E., Shioda, T., 2023. SARS-CoV-2 related antibody-dependent enhancement phenomena in vitro and in vivo. *Microorganisms* 11, 1015. <https://doi.org/10.3390/MICROORGANISMS11041015>, 2023, Vol. 11, Page 1015.
- Offen, D., Gilgun-Sherki, Y., Barhum, Y., Benhar, M., Grinberg, L., Reich, R., Melamed, E., Atlas, D., 2004. A low molecular weight copper chelator crosses the blood-brain barrier and attenuates experimental autoimmune encephalomyelitis. *J. Neurochem.* 89, 1241–1251. <https://doi.org/10.1111/j.1471-4159.2004.02428.x>.
- Ou, X., Liu, Y., Lei, X., Li, P., Mi, D., Ren, L., Guo, L., Guo, R., Chen, T., Hu, J., Xiang, Z., Mu, Z., Chen, X., Chen, J., Hu, K., Jin, Q., Wang, J., Qian, Z., 2020. Characterization of spike glycoprotein of SARS-CoV-2 on virus entry and its immune cross-reactivity with SARS-CoV. *Nat. Commun.* <https://doi.org/10.1038/s41467-020-15562-9>.
- Pfaff, A.R., Beltz, J., King, E., Ercal, N., 2020. Medicinal thiols: current status and new perspectives. *Mini Rev. Med. Chem.* 20, 513. <https://doi.org/10.2174/1389557519666191119144100>.
- Pinter, A., Kopelman, R., Li, Z., Kayman, S.C., Sanders, D.A., 1997. Localization of the labile disulfide bond between SU and TM of the murine leukemia virus envelope protein complex to a highly conserved CWLC motif in SU that resembles the active-site sequence of thiol-disulfide exchange enzymes. *J. Virol.* 71, 8073–8077.
- Pisoschi, A.M., Pop, A., Iordache, F., Stanca, L., Geicu, O.I., Bilteanu, L., Serban, A.I., 2022. Antioxidant, anti-inflammatory and immunomodulatory roles of vitamins in COVID-19 therapy. *Eur. J. Med. Chem.* <https://doi.org/10.1016/j.ejmech.2022.114175>.
- Plaper, T., Aupič, J., Dekleva, P., Lapenta, F., Keber, M.M., Jerala, R., Benčina, M., 2021. Coiled-coil heterodimers with increased stability for cellular regulation and sensing SARS-CoV-2 spike protein-mediated cell fusion. *Sci. Rep.* 11, 1–16. <https://doi.org/10.1038/s41598-021-88315-3>.
- Saito, A., Irie, T., Suzuki, R., Maemura, T., Nasser, H., Uriu, K., Kosugi, Y., Shirakawa, K., Sadamasu, K., Kimura, I., Ito, J., Wu, J., Iwatsuki-Horimoto, K., Ito, M., Yamayoshi, S., Loeber, S., Tsuda, M., Wang, L., Ozono, S., Butlertanaka, E.P., Tanaka, Y.L., Shimizu, R., Shimizu, K., Yoshimatsu, K., Kawabata, R., Sakaguchi, T., Tokunaga, K., Yoshida, I., Asakura, H., Nagashima, M., Kazuma, Y., Nomura, R., Horisawa, Y., Yoshimura, K., Takaori-Kondo, A., Imai, M., Chiba, M., Furihata, H., Hasebe, H., Kitazato, K., Kubo, H., Misawa, N., Morizako, N., Noda, K., Oide, A., Suganami, M., Takahashi, M., Tsushima, K., Yokoyama, M., Yuan, Y., Tanaka, S., Nakagawa, S., Ikeda, T., Fukuhara, T., Kawaoka, Y., Sato, K., 2022. Enhanced fusogenicity and pathogenicity of SARS-CoV-2 Delta P681R mutation. *Nature* 602, 300–306. <https://doi.org/10.1038/s41586-021-04266-9>.
- Shi, Y., Zeida, A., Edwards, C.E., Mallory, M.L., Sastre, S., Machado, M.R., Pickles, R.J., Fu, L., Liu, K., Yang, J., Baric, R.S., Boucher, R.C., Radi, R., Carroll, K.S., 2022. Thiol-based chemical probes exhibit antiviral activity against SARS-CoV-2 via allosteric disulfide disruption in the spike glycoprotein. *Proc. Natl. Acad. Sci. U. S. A.* 119 <https://doi.org/10.1073/pnas.2120419119>.
- Singh, J., Dhindsa, R.S., Misra, V., Singh, B., 2020. SARS-CoV2 infectivity is potentially modulated by host redox status. *Comput. Struct. Biotechnol. J.* 18, 3705–3711. <https://doi.org/10.1016/j.csbj.2020.11.016>.
- Sturman, L.S., Ricard, C.S., Holmes, K.V., 1990. Conformational change of the coronavirus peplomer glycoprotein at pH 8.0 and 37 degrees C correlates with virus aggregation and virus-induced cell fusion. *J. Virol.* 64, 3042–3050. <https://doi.org/10.1128/jvi.64.6.3042-3050.1990>.
- Suhail, S., Zajac, J., Fossom, C., Lowater, H., McCracken, C., Severson, N., Laatsch, B., Narkiewicz-Jodko, A., Johnson, B., Liebau, J., Bhattacharyya, S., Hati, S., 2020. Role of oxidative stress on SARS-CoV (SARS) and SARS-CoV-2 (COVID-19) infection: a review. *Protein J.* 39, 644–656. <https://doi.org/10.1007/s10930-020-09935-8>.
- van Eijk, L.E., Tami, A., Hillebrands, J.L., Den Dunnen, W.F.A., de Borst, M.H., van der Voort, P.H.J., Bulthuis, M.L.C., Veloo, A.C.M., Wold, K.I., Vincenti González, M.F., van der Gun, B.T.F., van Goor, H., Bourgonje, A.R., 2021. Mild coronavirus disease 2019 (Covid-19) is marked by systemic oxidative stress: a pilot study. *Antioxidants* 10. <https://doi.org/10.3390/antiox10122022>.
- Wallin, M., Ekström, M., Garoff, H., 2004. Isomerization of the intersubunit disulfide-bond in Env controls retrovirus fusion. *EMBO J.* 23, 54–65. <https://doi.org/10.1038/sj.emboj.7600012>.
- Wiesen, T., Atlas, D., 2022. Novel anti-apoptotic L-DOPA precursors SuperDopa and SuperDopamine as potential neuroprotective agents for halting/delaying progression of Parkinson's disease. *Cell Death Dis.* 13 <https://doi.org/10.1038/s41419-022-04667-2>.
- Yamasoba, D., Kimura, I., Nasser, H., Morioka, Y., Nao, N., Ito, J., Uriu, K., Tsuda, M., Zahradnik, J., Shirakawa, K., Suzuki, R., Kishimoto, M., Kosugi, Y., Kobiyama, K., Hara, T., Toyoda, M., Tanaka, Y.L., Butlertanaka, E.P., Shimizu, R., Ito, H., Wang, L., Oda, Y., Orba, Y., Sasaki, M., Nagata, K., Yoshimatsu, K., Asakura, H., Nagashima, M., Sadamasu, K., Yoshimura, K., Kuramochi, J., Seki, M., Fujiki, R., Kaneda, A., Shimada, T., Nakada, T. aki, Sakao, S., Suzuki, T., Ueno, T., Takaori-Kondo, A., Ishii, K.J., Schreiber, G., Sawa, H., Saito, A., Irie, T., Tanaka, S., Matsuno, K., Fukuhara, T., Ikeda, T., Sato, K., 2022. Virological characteristics of the SARS-CoV-2 Omicron BA.2 spike. *Cell.* <https://doi.org/10.1016/j.cell.2022.04.035>.
- Yang, Y., Xu, F., 2022. Evolving Understanding of Antibody-dependent Enhancement (ADE) of SARS-CoV-2. <https://doi.org/10.3389/fimmu.2022.1008285>.
- Ye, Y., 2023. China's rolling COVID waves could hit every six months — infecting millions. *Nature.* <https://doi.org/10.1038/d41586-023-01872-7>.
- Žarković, N., Jastrzab, A., Jarocka-Karpowicz, I., Orehovec, B., Baršić, B., Tarle, M., Kmet, M., Luksić, I., Łuczaj, W., Skrzydlewska, E., 2022. The impact of severe COVID-19 on plasma antioxidants. *Molecules* 27, 5323. <https://doi.org/10.3390/molecules27165323>.
- Zhou, Y.W., Xie, Y., Tang, L.S., Pu, D., Zhu, Y.J., Liu, J.Y., Ma, X.L., 2021. Therapeutic targets and interventional strategies in COVID-19: mechanisms and clinical studies. *Signal Transduct. Targeted Ther.* 6 <https://doi.org/10.1038/s41392-021-00733-x>.